Pergamon

Journal of Structural Geology, Vol. 16, No. 12, pp. 1619 to 1639, 1994

0191-8141/94 $7.00+0.00

0191-8141(94)E0012-N

The opening of the Gulf of California near Loreto, Baja California, Mexico: from basin and range extension to transtensional tectonics

ANDREA ZANCHI

Dipartimento di Scienze della Terra, Via Mangiagalli 34-20133, Milano, Italy

(*Received* 19 *October* 1992; *accepted in revised form* 27 *January* 1994)

Abstract—Detailed structural field analyses of faults and fractures have led to the reconstruction of the tectonic evolution of the Loreto region (Baja California, Mexico) during the opening of the Gulf of California. Three main tectonic events have been recognized: (i) formation of large-scale radial structures along the future Main Gulf Escarpment, here interpreted as associated with emplacement of magmatic bodies at shallow levels during the beginning of extension processes in Early–Middle Miocene; (ii) NE–SW extension (Basin and Range event) active since 15 Ma, producing NW–SE normal dip-slip faults in the Oligo-Miocene volcaniclastic basement, and indicating high extension rates; (iii) transtensional tectonics recorded especially in the Plio-Quaternary sediments and associated with the activation of NW–SE dextral strike-slip faults and N–S normal faults. The tectonic structures related to the Basin and Range extension are sealed by the Plio-Quaternary sediments of the Loreto basin and by the volcanics of the Mencenares Volcanic Complex, a huge volcanic field interfingering with the sedimentary succession of the basin.

INTRODUCTION

THE opening of the Gulf of California has evolved through a complex history related to the Neogene geodynamic evolution of the North American Plate (Stock & Hodges 1989, Lonsdale 1991). Several oceanographic surveys have shed light on the structure of the submerged portion of the Gulf (Fig. 1) and on the plate kinematics within the region (Rusnack *et al.* 1964, Moore & Buffington 1968, Atwater 1970, Larson 1972, Larson *et al.* 1972, Moore 1973, Bischoff *et al.* 1974, Klitgord *et al.* 1974, Mammerickx & Klitgord 1982, Couch *et al.* 1991, Lyle & Ness 1991). Particular attention has been devoted to the evolution of the Neogene–Quaternary magmatism in the Baja California peninsula (Gastil *et al.* 1975, 1979, Hausback 1984, Sawlan & Smith 1984, Saunders *et al.* 1987, Sawlan 1991). Analyses of fault mechanisms in Late Miocene–Quaternary rocks along the Gulf have been performed by Angelier *et al.* (1981) and by Colletta & Angelier (1983), who recognized two main deformational events, as already suggested by Karig & Jensky (1972): (i) an early extensional phase related to the Basin and Range tectonics involving the Gulf region during the Late Miocene; (ii) a successive activation of the transform plate boundary between the North American and the Pacific Plate in the Gulf since 3.5 Ma.

A large region of Baja California extending from Loreto to La Purisima has been studied by a team of Italian geologists, in order to unravel the Neogene–Quaternary evolution of the peninsula. Detailed work has been carried out in the Loreto area, located south of Bahia Conception, where Pliocene marine sediments are interbedded with the Mencenares Volcanic Complex (MVC), a large volcanic field developed within the Rift. Geological mapping (Zanchi 1989b) has been performed in the Loreto basin and in the MVC (Bigioggero *et al.* 1992 in review), to reconstruct the evolution of the region during Plio-Quaternary times (Fig. 2).

In this paper the results of structural analyses of faults related to the opening of the Gulf are presented. These structural analyses have focussed on the Early Miocene

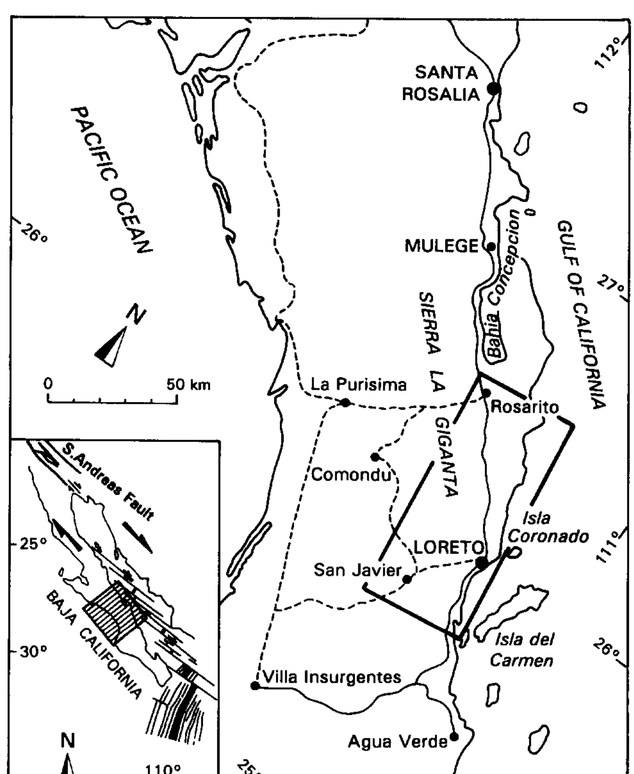

Fig. 1. Location map of the Gulf of California and of the study area (rectangle around Loreto).

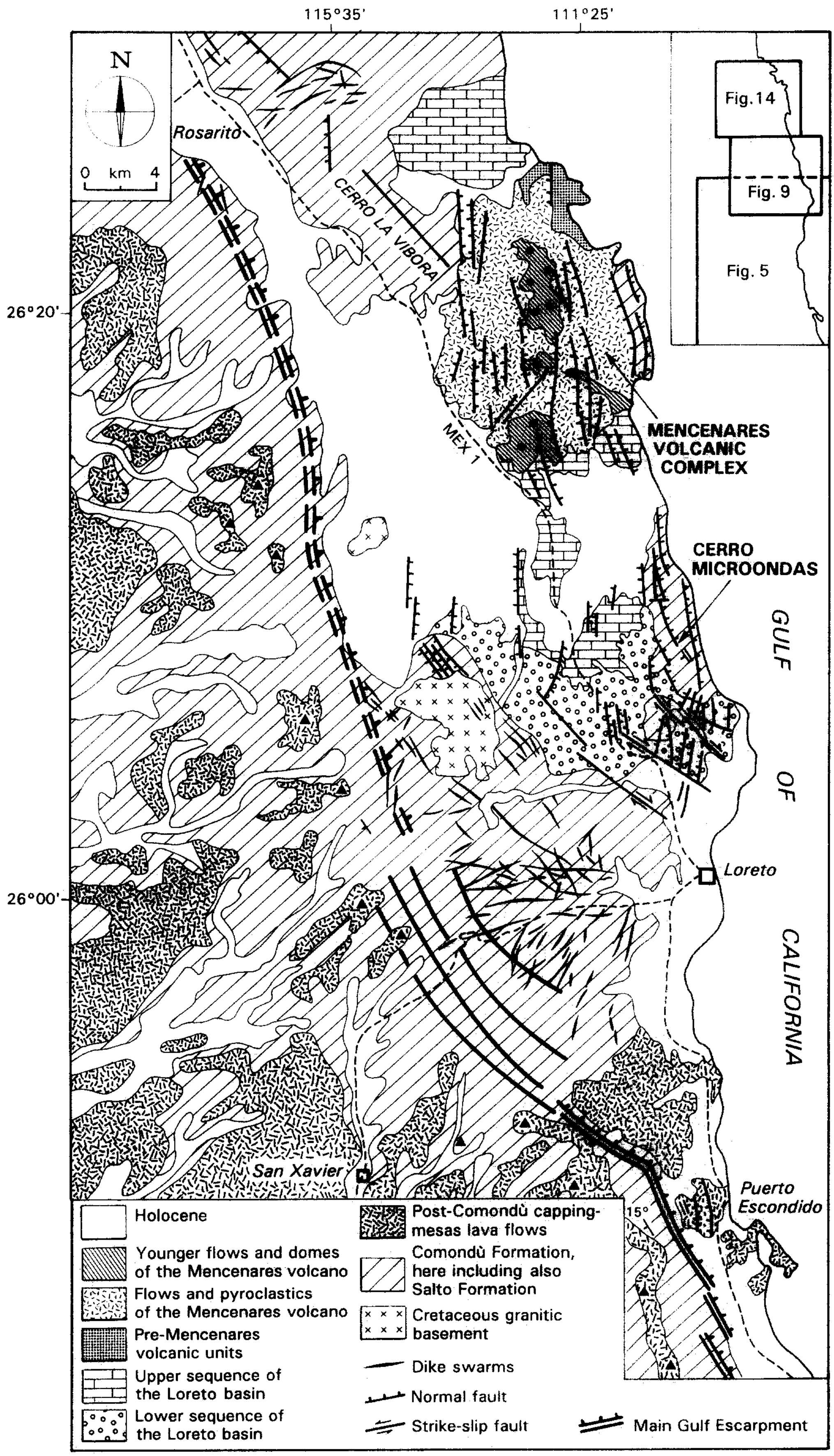

Fig. 2. Index geological map of the Loreto region. Inset shows locations of Figs. 5, 9 & 14.

volcaniclastic basement pre-dating the Gulf opening and on the successive Plio-Quarternary successions of the Loreto basin and of the MVC.

THE OPENING OF THE GULF OF CALIFORNIA

The opening of the Gulf of California and the formation of a marine basin, named 'Protogulf of California' (Karig & Jensky 1972) dates at about 10 Ma, as inferred from field evidence collected by many authors in several areas around the Sea of Cortez (Gastil *et al.* 1975, 1979, Boehm *et al.* 1984, Ortlieb & Colletta 1984, Stock & Hodges 1989, Smith 1991). The opening of the Protogulf also coincides with a change in the geochemistry of the volcanic products, from calcalkaline to transitional-calcalkaline and Mg-high, K_2O rich andesites, occurring at about 12–10 Ma (Hausback 1984, Sawlan & Smith 1984, Saunders *et al.* 1987, Sawlan 1991).

These rifting phenomena were interpreted as related to the Basin and Range extension (Angelier *et al.* 1981, Dokka & Merriam 1982, Colletta & Angelier 1983), which affected the north-western portion of Mexico during this period. The opening of the Protogulf induced intense tectonic extension, at least 40%, as pointed out by Colletta & Angelier (1983). The direction of extension was mainly NE–SW along the eastern coast of Baja California and in the Sonora coast, on the other side of the Gulf. During extension a deep marine basin, bounded by strongly extended and tilted blocks of continental crust, formed between the Baja peninsula and mainland Mexico.

The successive activation of a complex transform plate boundary within the Gulf, connecting the San Andreas Fault System with the East Pacific rise, has been dated at about 3.5 Ma (Larson *et al.* 1968, 1972, Mammerickx & Klitgord 1982, Lonsdale 1991, Lyle & Ness 1991), and has caused the peninsula to move 260 km to the north, as also suggested by paleomagnetic results (Hagstrum *et al.* 1987). This triggered the Gulf to become the Pacific–North American transform plate boundary, replacing the Tosco–Abreojos and San Benito transform fault system, located off-shore the western coast of the Baja California peninsula in the continental borderland (Spencer & Normark 1979). Dextral strike-slip motion along transform faults and associated formation of pull-apart basins, where oceanic crust is produced, have occurred in the Gulf. The main transform faults trend NW–SE and are partly inherited from the Protogulf structures. Along the eastern coast of the peninsula the deformation produced by the dextral shearing is mainly represented by en échelon N–S striking normal faults and NNW–SSE to NW–SE striking dextral strike-slip and oblique faults (Angelier *et al.* 1981), related to a clockwise rotation of the direction of extension from NE–SW to E–W. This tectonic scenario has been recently confirmed by a geodetic network established across the Gulf, indicating an average dextral motion of 8 ± 3 cm y^{-1} between the two sides of the central part of the Gulf (Ortlieb *et al.* 1989).

GEOLOGICAL FRAMEWORK OF THE LORETO REGION

The Loreto region is located in the southern part of the Baja California peninsula along the west escarpment of the Gulf of California, formed by the high range, the Sierra de La Giganta. The Cretaceous granitic basement, outcropping northwest of Loreto, is covered by a thick volcaniclastic succession of Late Oligocene–Middle Miocene age (Fig. 2). At the foot of the Sierra de La Giganta the Cretaceous basement is covered by cross-bedded sandstones with ignimbritic tuffs referrable to the Salto Formation of McFall (1968), and dated at 29 Ma in the Loreto area (McLean 1988). The Salto Formation, related to the Sierra Madre Occidental volcanic activity, is in turn covered by a thick succession, the Comondù Formation s.s. (McFall 1968, Gastil *et al.* 1975, 1979, Hausback 1984). This formation consists of fluviatile volcaniclastics, andesitic breccias and lava flows, representing the products of the Miocene calc-alkaline arc located in the Gulf region. Gastil *et al.* (1979) obtained K/Ar ages ranging between 23 and 17 Ma in two different sections along the Sierra. Several andesitic dikes, cutting the whole sequence, have been dated, yielding ages between 23 and 15 Ma (Gastil *et al.* 1979, McLean *et al.* 1987, McLean 1988). Other authors obtained different radiometric ages of 7.6 ± 5.5 Ma (Piscke 1979: in Hagstrum *et al.* 1987) for the same intrusives. In the Loreto area the Comondù Formation is covered by younger lava flows of 15 to 6 Ma (Gastil *et al.* 1979), coeval to the lava flows at the top of the Sierra (Hausback 1984, McLean *et al.* 1987). Some of the oldest flows which cap the Comondù Formation are downfaulted along the main scarp, giving a minimum age for the opening of the Protogulf.

As a consequence of rifting phenomena, a marine basin developed north of Loreto (Fig. 2) between the Main Gulf Escarpment and the strongly tilted blocks of the Comondù Formation (McLean 1988, Zanchi *et al.* 1988). The basin contains several hundreds of meters of marine sediments, deposited during the opening of the Gulf of California. Two sedimentary sequences separated by an unconformity have been recognized within the basin (Zanchi *et al.* 1988, Zanchi 1989a,b, Zanchi *et al.* in preparation). The lower sedimentary sequence lies, with a strong angular unconformity, on tilted blocks consisting of the Comondù Formation, and is composed of debris-flow dominated fan-delta units laterally and upwardly evolving to a thick shallow-sea fossiliferous unit. The upper sequence contains bioclastic and terrigenous units and is clearly transgressive on the margins of the basin. Pectinid assemblages collected in the lower sequence are no older than Pliocene (Robba & Piazza 1992, pers. comm.), whereas Foraminifera microfauna at the top of the upper sequence are Late Pliocene in age (Zone N21, Gelati & Valdisturlo 1992, pers. comm.). These data confirm the radiometric ages obtained by McLean (1988), indicating 1.9–3.3 Ma ages for the volcanic layers interbedded in the Loreto sediments. Sedimentation in the basin was coeval with the intensive

Table 1. Information on stress tensor determinations obtained in the Loreto region. In the table are reported: reference number (Site), location (Lat. N, Long. W, in degrees), stress axes ($\sigma1$, $\sigma2$, $\sigma3$) in trend/plunge, ratio between principal stress differences $\Phi = (\sigma2 - \sigma3)/(\sigma1 - \sigma3)$ (Angelier, 1984), number of fault planes (N) and averages angle between computed shear stress and actual slip in degrees (D). All the sites are in the Comondù Formation, with the exception of sites R16 and R2Tot which are located in the Loreto basin sediments

Formation of radial structures

Site	Lat.	Long.	$\sigma1$	$\sigma2$	$\sigma3$	Φ	*N*	*D*
L9BIS	25-51-38	111-22-21	158/85	274/02	004/05	0.00	29	8.7
L38	25-53-38	111-25-30	187/82	279/01	009/07	0.03	19	4
L53	25-54-17	111-26-20	182/81	019/08	288/02	0.1	14	4.7
L54	25-54-03	111-26-30	123/85	267/04	358/02	0.05	21	5.4
L55	25-54-26	111-26-42	339/89	109/01	199/01	0.08	16	8.2
L57D	26-00-34	111-26-48	166/85	287/03	018/04	0.04	30	7.2
L59	26-10-33	111-34-22	322/89	103/01	194/01	0.06	13	5.4
L65	25-31-17	111-05-43	146/86	293/03	023/02	0.06	7	3.7
L66	25-30-42	110-09-42	277/82	034/03	124/07	0.08	19	8.3
L67	25-32-41	110-89-36	231/63	076/25	342/01	0.33	4	5
L68	25-34-17	110-10-48	290/83	065/05	156/05	0.33	15	6
L70	26-05-17	111-27-00	161/85	060/01	330/04	0.05	13	11

Basin and Range extension

Site	Lat.	Long.	$\sigma1$	$\sigma2$	$\sigma3$	Φ	*N*	*D*
L4	25-58-34	111-28-17	239/76	145/01	054/13	0.06	42	4.1
L5D	25-59-00	111-28-38	015/76	150/09	241/09	0.14	14	5.9
L9	25-51-38	111-22-21	058/71	152/01	243/18	0.05	21	7.3
L10	25-51-38	111-22-22	039/74	134/01	224/15	0.07	14	6.7
L20	26-11-47	111-31-28	286/79	136/09	045/05	0.04	13	4.6
L60	26-11-47	111-31-28	139/84	324/06	234/01	0.07	19	7.8
L69	26-30-00	111-34-00	241/87	134/01	044/03	0.11	24	4.8

Pliocene–Quaternary transtension

Site	Lat.	Long.	$\sigma1$	$\sigma2$	$\sigma3$	Φ	*N*	*D*
L5C	25-59-00	111-28-38	159/17	359/72	251/06	0.11	12	6.2
L54C	25-54-26	111-26-42	179/04	050/83	269/05	0.29	9	10.5
L57C	26-00-34	111-26-48	353/03	103/81	262/08	0.07	18	11
R2TOT	26-04-40	111-26-48	356/67	181/21	090/02	0.07	12	7.9
R16	26-05-20	111-24-05	005/11	225/75	097/09	0.02	6	6.8

volcanic activity developed in the Mencenares Volcanic Complex, a huge volcanic field located 30 km north of Loreto, as indicated by the presence of reworked pyroclastics in both the sequences and interfingering between marine sediments and volcanics in the upper sequence.

METHODOLOGY

The study of fault planes was carried out using analytical techniques with the purpose to reconstruct the evolution of paleostress fields (following Carey 1979, Angelier 1984, Angelier *et al.* 1985). Assuming that the maximum shear stress on a fault plane is parallel to the observed striation, an average stress deviator can be computed minimizing the angle between the measured striation and the theoretical direction of the maximum shear stress, when at least four fault planes with different orientations are available. The algorithm proposed by Carey (1979) and her computer program have been used in this work. The program gives the eigenvalues and eigenvectors of the average deviator and the angle between the observed and the calculated striations. Stress tensors were determined in about 20 sites (Table 1). The sense of motion of fault planes was established in the field using kinematic indicators following Petit *et al.* (1987). The chronology among polyphase structures was established using geometric criteria (e.g. superposed slickenside lineations or geometric intersections among different fault planes).

About 1500 fractures, including faults with no slickensides, joints and tension gashes were also analyzed, using the relationships between stress and simple brittle structures, suggested by Hancock (1985). Joints and tension gashes were mainly studied in sandstones of the Comondù Formation outcropping in the interior of the peninsula, where deformation was generally weak. In order to check the reliability of the results obtained from the analysis of mesoscopic faults (Hancock 1985), they were compared with the kinematics of major structures and with the geological evolution of the region. Photogeological techniques for structural interpretation have also been used to describe the complex regional fracture pattern recognized along the Main Gulf Escarpment.

THE GEOMETRY OF FAULTS AND STRUCTURES

The field analysis of faults and other structures was carried out in the Comondù and Salto Formations and in

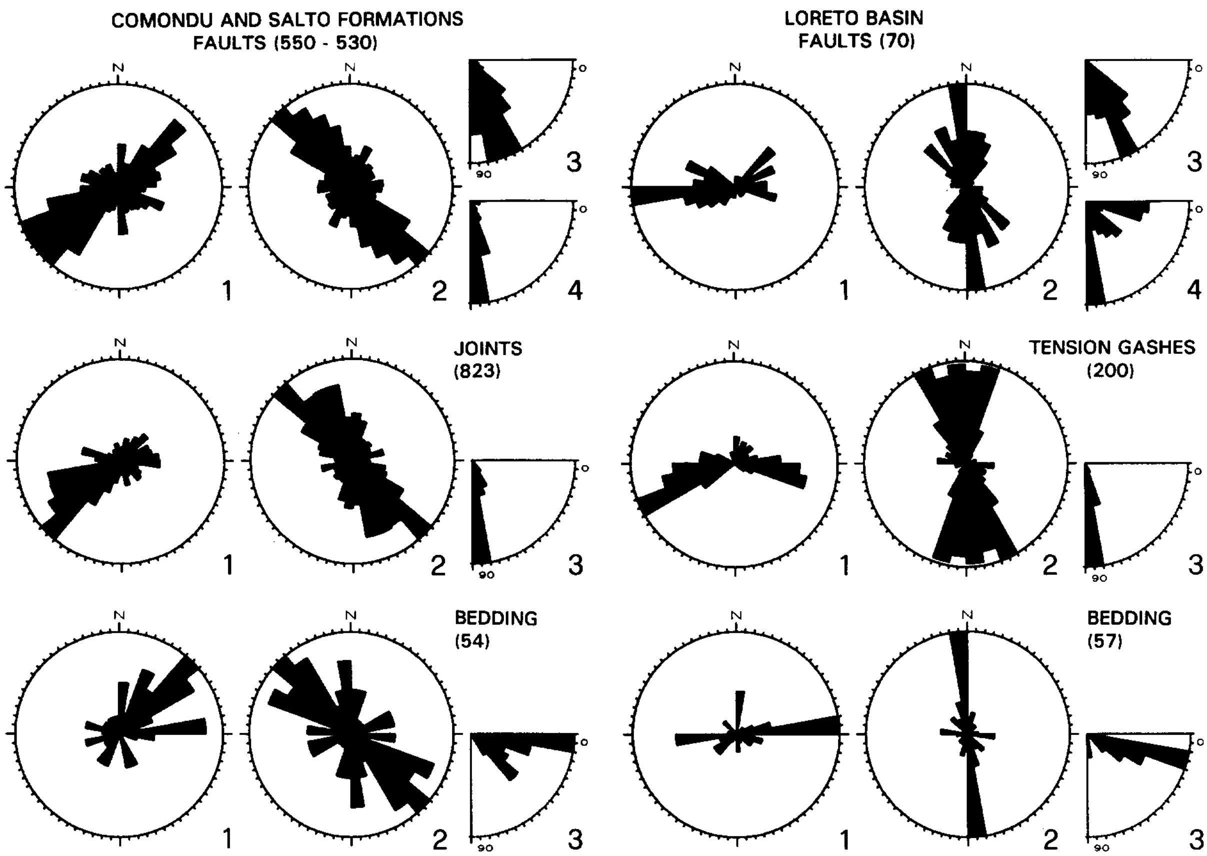

Fig. 3. Rose diagrams for the structures observed in the Comondù and Salto Formations (left side) and in the Loreto basin sediments (right side). The radius of the rose corresponds to the class with the highest frequency. (1) Dip direction; (2) strike; (3) dip; and (4) pitch (angle between the striation and the horizontal as measured in the fault plane).

the Loreto basin sediments (Fig. 3), which thus separate the observed fault populations on a stratigraphic basis. Simple statistics was applied to the geometrical characteristics of structures, following Angelier *et al.* (1985).

About 550 faults with slickensides were measured along the Main Gulf Escarpment in the Loreto region from Rosarito to Agua Verde (Fig. 1), and in tilted blocks constituted by the Comondù and Salto Formations. Rose diagrams have been drawn for faults, joints and bedding planes. The strikes of the faults show a large NW–SE peak (120°–170°), which corresponds to the regional trend of the rift escarpment south of Loreto, and also corresponds to the strike of the faults present in the tilted blocks outcropping along the flanks of the Loreto basin. These NW–SE faults are mostly antithetic with respect to the Main Gulf Escarpment, as indicated by the geometry of rotated blocks. The dips of the fault planes are generally high, and typical of normal or strike-slip faults. Pitches indicate nearly pure dip-slip motion (80°–90°) for most faults, with oblique and strike-slip motions subordinate. The strikes of the joints (823) are very similar to the strike of fault planes; joints are almost vertical (80°–90°), and are related to tension or hybrid shear fracturing, according to the classification of Hancock (1985). The strike of bedding shows two mean directions: NW–SE and N–S with northeastwards and eastwards dipping. The dip is generally high, up to 55° in rotated blocks, suggesting the activation of listric faults during the opening of the Protogulf Rift. Low tilts correspond to attitudes of the strata located west of the escarpment, where the Comondù Formation is generally subhorizontal. Bed tilting is mainly consistent with the rotation caused by the NW–SE normal dip-slip faults, as also suggested by the fault plane dip directions.

Fractures measured in the Loreto basin and in the Mencenares Volcanic Complex display very different geometries. Only 70 planes with striations were found in a total population of about 300 faults. Most of the striated planes correspond to large mapped structures, allowing a representative kinematic reconstruction of fault motions which occurred in the basin. The rose diagram relative to the strike of the striated fault shows a strong N–S peak, together with NW–SE to NNW–SSE minor peaks. Dip values are characteristic of normal and strike-slip faults. The pitch distribution shows three separate peaks, representing dip-slip, strike-slip and oblique-slip motions. Tension gashes (200) have a large and uniform strike distribution ranging from NNW–SSE to NNE–SSW. The rose diagrams relative to bedding are also significant: in the Comondù Formation block rotation is mainly due to NW–SE faults and subordinately to N–S faults, whereas in the Loreto basin tilting is related to N–S trending normal faults, as suggested by the dip direction of bedding. The dip of the Loreto basin sediments is between 10° and 30°, but can locally reach more than 40°.

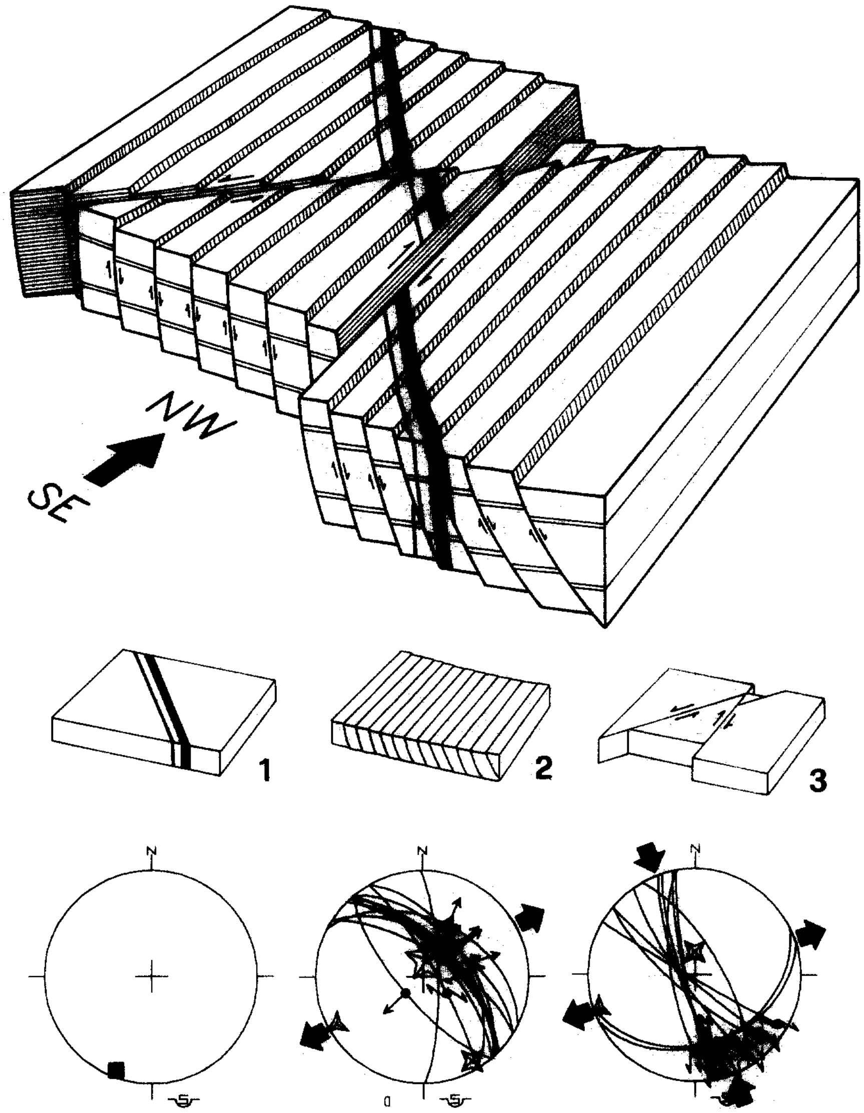

Fig. 4. Block-diagram illustrating the geometrical relationships among the structures recognized in the Comondù Formation at site L5, located near El Pilon de Las Parras (road from Loreto to San Xavier): (1) dike emplacement; (2) NE–SW (Protogulf) extension; and (3) NNW–SSE compression with formation of strike-slip faults (small thrust faults have been omitted in the block-diagram). Schmidt's projection of lower hemisphere. Faults are great circles, slickenside lineations are dots with arrows indicating the sense of motion of the hangingwall. Stress axes are represented as stars with five ($\sigma1$), four ($\sigma2$) and three branches ($\sigma3$). Large divergent black arrows indicate the horizontal direction of $\sigma3$, convergent arrows the horizontal direction of $\sigma1$. Black squares are poles to dikes.

DEFORMATION IN THE COMONDÙ AND SALTO FORMATIONS

Most of the observed faults were measured in the lower volcaniclastic units of the Comondù Formation outcropping along the base of the Main Gulf Escarpment. Data were also collected in the tilted blocks east of the scarp. Stress tensors were determined in about 20 sites (Table 1); faults without slickensides and joints were analyzed in another 50 sites.

Three main tectonic events were recognized within the Comondù succession, and are schematically represented by the geometrical superposition of structures found at site L5 (Fig. 4). At this site the succession of the structural events is as follows. The emplacement of ENE–WSW subvertical dike (1) is followed by the nucleation of NW–SE normal faults (2), and finally conjugate sets of strike-slip faults associated with small thrusts, displacing the dike (3). Reactivation of the normal faults by strike-slip movement has been observed. The same succession of events has been recognized in many other sites: NW–SE normal faults generally displace dikes, and, where polyphase fault associations are seen, oblique or strike-slip striations post-date dip-slip motions.

Dike emplacement associated with the formation of radial structures

A very intensive and penetrative fracture pattern, related to the main escarpment of the Gulf, has been detected by aid of photogeological interpretation and field analysis. Kilometre-scale dike swarms and complex sets of fractures arranged with a radial pattern, associated with subcircular concentric faults and joints, seem to coexist with the NNW–SSE to NW–SE fracture sys-

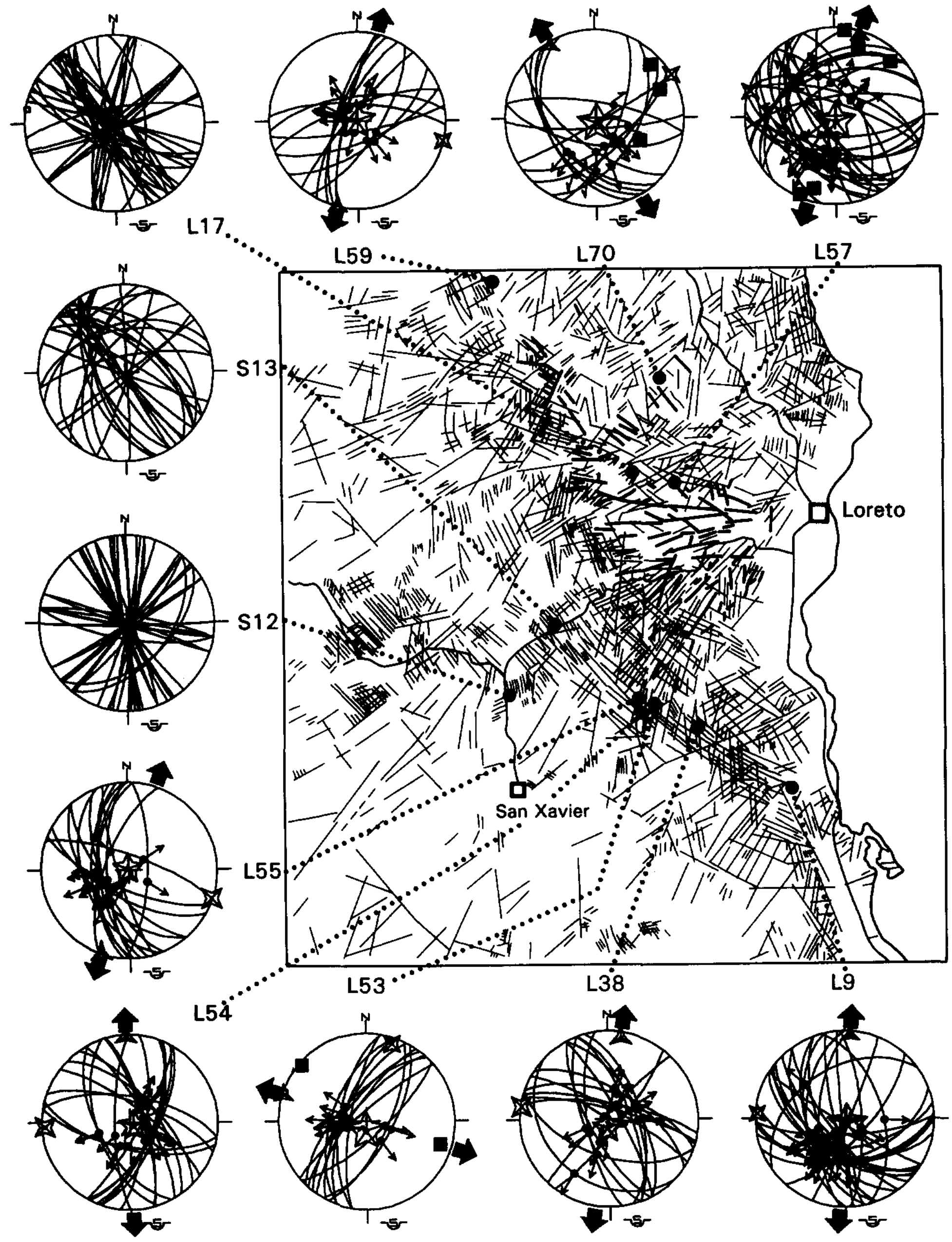

Fig. 5. General structural scheme of the Loreto radial structure and associated mesoscopic fracture assemblages observed in the field with relative stress tensor determinations. Fracture systems have been identified mainly through photogeological interpretations. Thin lines are fractures, solid black lines are major dikes. Symbols as in Fig. 4; great circles at sites L17, S12 and S13 are joints. Map outline indicated on Fig. 2.

tems developed along the Main Gulf Escarpment. Just west of the town of Loreto the Gulf escarpment becomes subcircular in association to a well defined radial system of large vertical dikes and small subvolcanic bodies (Fig. 5). These radial and subcircular complexes crop out along the rift margin west and south of Bahia Conception, near Loreto and at Agua Verde. Such structures have been recognized only in the Comondù Formation, because elsewhere they are covered by the youngest, post-15 Ma (Gastil *et al.* 1979) lava flows. The fracture field is well developed for a few kilometres in the deep canyons west of the escarpment, where the Comondù Formation sandstones crop out under young lava flows.

Emplacement of the radial dike swarms is also connected with the formation of radial sets of faults always with pure dip-slip motions and with the formation of extensional-hybrid joints, which also cross the dikes and their contacts. Most of the fractures are parallel to the main dikes. Faults perpendicular to the radial sets bear dip-slip striations and are parallel to the subcircular concentric faults. Stress tensors obtained at about ten sites indicate that the $\sigma1$ axis is always vertical and the $\sigma3$ axis is horizontal. The direction of the $\sigma3$ axis is generally poorly defined, its eigenvalue being very close to the $\sigma2$ value (Table 1, see ratio Φ), causing substitution between the horizontal stress axes in nearby sites (Fig. 5: Loreto structure: Fig. 6; Agua Verde structure). This is probably due to local stress field variations occurring during dike swarm emplacement related to the formation of the radial structures. In some cases the computed $\sigma3$ axis is perpendicular to the $\sigma3$ axis shown by the large andesitic dikes (Figs. 5 and 6). Joints measured inside

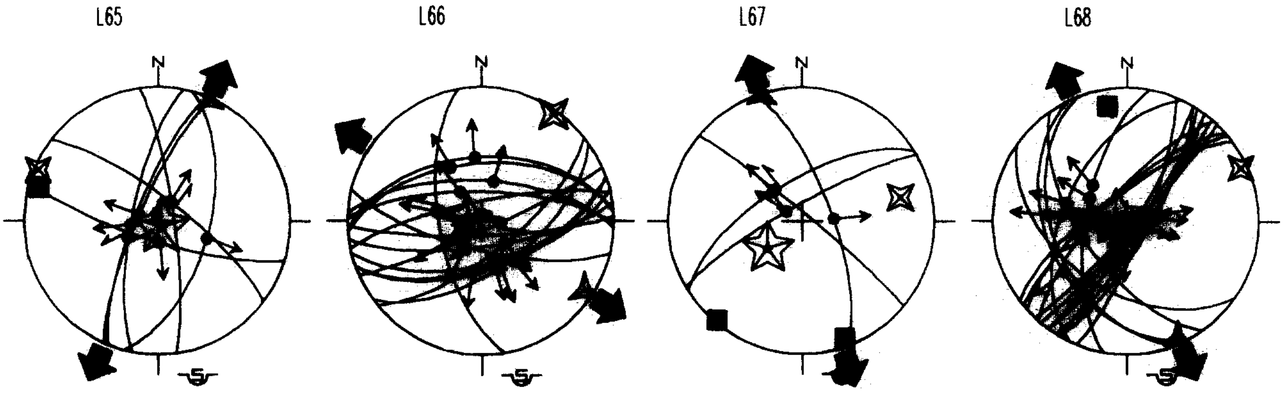

Fig. 6. Examples of fault populations and relative stress tensor determinations observed within the radial structure of Agua Verde located in Fig. 1. Symbols as in previous figures.

the radial structures also indicate the existence of radial and perpendicular vertical sets of extensional and hybrid joints following the trends shown by the main dikes and by the fault systems (Fig. 5).

Basin and Range extension (Protogulf opening)

The most common fault assemblage found along the escarpment of the Gulf consists of a NW–SE trending system of conjugate normal faults with dip-slip motions, locally associated with normal faults with different trends. In Fig. 7 examples of fault associations and relative stress tensors are reported: the $\sigma1$ axis is vertical and the $\sigma3$ axis is subhorizontal and trends NE–SW. Fracture systems in tilted blocks show a similar direction of $\sigma3$, as indicated by the geometry of conjugate fault and joint sets developed before block rotation (Fig. 7: L11 and L19). At both sites L11 and L19 block-tilting up to 50° occurred, due to rotation along antithetic faults formed near the rift main boundary fault. High angle reverse faults are due to tilting of previously formed normal faults. After block rotation had occurred, the generation of new faults with the same direction developed at site L19. Also NW–SE trending dike swarms, similar to those intruded in the radial structures, are rotated showing that emplacement occurred when bedding was horizontal. Fault assemblages related to the Loreto radial structure are also tilted, due to rotation along successive NW–SE normal faults. Mesoscopic faults are generally parallel to the Main Gulf Escarpment and to tilted blocks developed to the east, between Puerto Escondido and the southern part of the Loreto basin, where Basin and Range structures are well preserved.

Interaction between the radial systems of fractures and the NW–SE extensional faults related to the Protogulf opening can be sometimes detected, as for sites L9BIS and L57D (Fig. 5), placed within the Loreto radial structure. In fact, here, it was not possible to establish a relative chronology among different slip surfaces. At site L57D, NW–SE normal faults cross the dikes, indicating that dike emplacement pre-dated the extension along NW–SE faults.

The NW–SE fracture systems, recognized within the peninsula through photoanalysis, correspond to closely spaced penetrative sets of vertical extensional or hybrid joints and tension gashes developed in the Comondù Formation sandstones. Joint populations are regular along the studied section through the whole peninsula, from San Javier to the Comondù region. In most of the observed sites, located up to 40 km west of the rift, NW–SE fractures of extensional type are dominant and are often associated with subperpendicular joints, probably due to substitution between the $\sigma2$ and $\sigma3$ axes.

The trace of the fault escarpment reported in Figs. 2 and 7 corresponds with the actual location of the western boundary fault of the Protogulf Rift present south of Loreto, where the attitude of the main fault seems to be subvertical. Here the main boundary fault juxtaposes the gently SW-dipping volcaniclastic sequences of the Comondù with a steeply NE dipping block containing the upper part of the Comondù beds and post-Comondù lava flows. West and north of Loreto, the escarpment is deeply eroded and its trace is covered by Quaternary alluvium. N–S trending active normal faults present at the base of the scarp suggest a recent reactivation of the structure due to E–W extension.

The Protogulf escarpment can be generally correlated to the break-away ridge or zone A of Wernicke (1985) and represents the western boundary of the Basin and Range Province. The attitude of tilted blocks underlying the Loreto basin sediments shows a counter-fan geometry (Gibbs 1984) near the major boundary fault; it may be due to sequential faulting occurring only in the hangingwall, moving above a listric detachment fault. Listric faults must also bound the rotated blocks, as a strong change of the dip of beds is noted through the basin. This zone can be tentatively related to the B zone of extensional allochthons of Wernicke (1985), where high rates of extension occur. The main significant difference is given by the sense of rotation of faults, which are almost antithetic in the Loreto basin section, with respect to the B zone of Wernicke (1985), where faults are synthetic.

The transtension

Strike-slip faults and small subordinate thrust faults have been observed together with the dip-slip normal

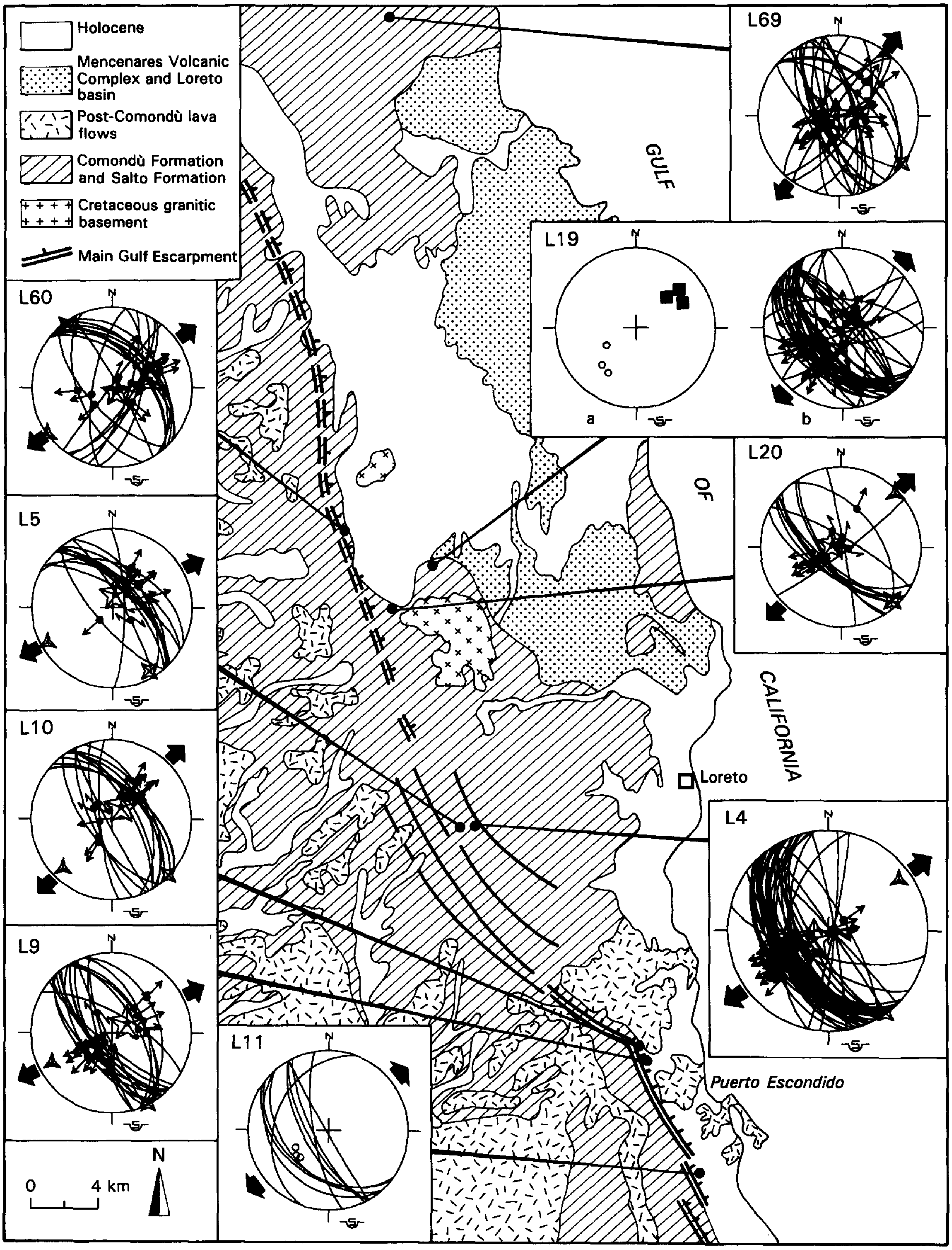

Fig. 7. Examples of fault populations and reduced stress tensors in the Comondù and Salto Formations relative to the Protogulf NE–SW extension (Basin and Range extension). Symbols as in previous figures. Small circles are poles to bedding; when omitted, bedding is subhorizontal.

fault assemblages of the Protogulf. At many sites NW–SE normal faults related to the Protogulf opening show superposed dextral or oblique-dextral striations; the relative chronology of striations always indicates that strike-slip and oblique movements took place later. Where polyphase fault populations were found, two different deviators were established, which explain at least the 75% of the total number of fault planes. The

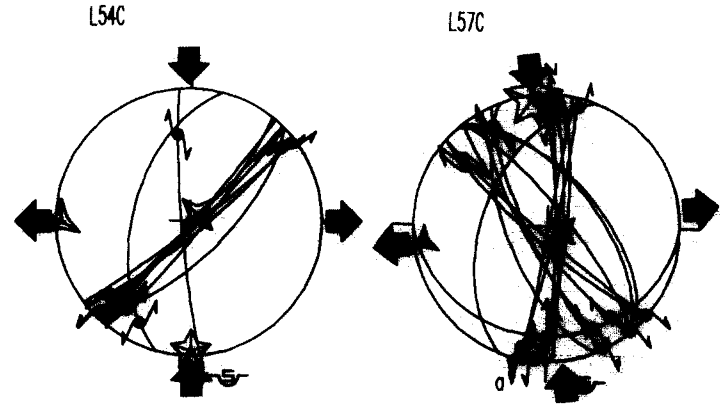

Fig. 8. Examples of fault populations relative to the N–S compression observed in the Comondù Formation. Symbols as in previous figures.

best solutions have given a vertical $\sigma 2$ axis, a N–S trending $\sigma 1$ axis and an E–W $\sigma 3$ axis, related to conjugate sets of NW–SE dextral and NE–SW to NNE–SSW strike-slip faults (Fig. 8). At site L5 sinistral and dextral strike-slip faults associated with small thrusts crosscut andesitic dikes with decametric net-slips (Fig. 4), indicating a horizontal NNW–SSE $\sigma 1$ axis and a horizontal slightly oblique ENE–WSW $\sigma 2$ axis. The anisotropy due to the penetrative normal fault systems of the Protogulf may be responsible for the rotation of the stress field. N–S tension gashes and joints, crossing the Protogulf structures and related to the successive E–W extension, were also measured in the Comondù beds in all the region.

DEFORMATION IN THE LORETO BASIN AND IN THE MENCENARES VOLCANIC COMPLEX

Deformation in the Loreto basin

The Loreto basin sediments crop out a few kilometres north of Loreto, forming a large NW–SE to N–S trending graben developed between the Main Gulf Escarpment and the Cerro Microondas Horst (Fig. 9). Marine sandstones deposited in the same basin crop out also north of the Mencenares Volcanic Complex. Detailed mapping and structural analyses have been mainly carried out between Mencenares and Loreto in an area of about 20 km^2. A schematic cross-section through the basin is shown in Fig. 10(a). It represents the general geometry of the Loreto basin sedimentary sequences. The architecture of the basin has been reconstructed on the basis of detailed mapping and stratigraphic work (Zanchi 1989b). Quaternary transtensional faults have been removed in order to give emphasis to the basin structure. Figure 10(b) shows a geological cross-section through the basin, and also takes into account post-sedimentary tectonic structures. The angular unconformity separating the lower sequence from the Comondù Formation tilted blocks is interpreted as the result of successive infilling of the basin developed after the opening of the Protogulf. The thick units of the lower sequence suggest strong tectonic subsidence due to synsedimentary activity along NW–SE trending faults, probably active as dextral or dextral-normal faults during the beginning of the transtension.

The two sedimentary sequences recognized in the basin (Fig. 9) show the same fault mechanisms, which are referrable to the last tectonic phase recognized in the underlying Comondù and Salto Formations. Figure 11 illustrates the kinematics of the major mapped faults obtained measuring the slip-vectors along them. N–S normal faults with dip-slip motion and NW–SE dextral strike-slip and dextral-normal oblique fault planes are dominant in the basin. This association is consistent with mesoscopic data, showing N–S trending normal dip-slip faults, NW–SE dextral strike-slip or oblique-normal faults; NE–SW sinistral strike-slip faults, although less common, have also been recognized. Normal faults are arranged with an en échelon pattern in the central part of the basin, strongly resembling the relay structures described by Larsen (1988), due to partially disconnected hangingwall moving on a listric fault plane. This is also suggested by the differential tilting and relative uplift of the Loreto basin sediments, due to listric geometry of the large E-dipping fault system (Fig. 10b) bounding the western flank of the Microondas Horst.

The structures found at sites R16 and R2 near the Rancho Piedras Rodadas along the Mex1 highway are the most complete fault associations with good kinematic indicators found in the sediments of the basin. They are related with the formation of a small pull-apart basin (Fig. 11) along the northern tip of a major NW–SE dextral strike-slip fault. At this site a conjugate system of strike-slip faults is associated with N–S trending normal faults, indicating a N–S horizontal $\sigma 1$ axis and a horizontal E–W $\sigma 3$ axis. Because of the general lack of striations on fault planes, these were the only places where the reduction of data was possible. At all the other sites stress directions were evaluated with simple geometrical criteria, using tension gashes or conjugate sets of faults and joints.

The associations of tension gashes, joints and normal faults indicate an E–W trending $\sigma 3$, in agreement with dip-slip motions along N–S trending faults. Conjugate sets of strike-slip faults suggest a N–S horizontal $\sigma 1$ and an E–W trending $\sigma 3$. NW–SE faults often display com-

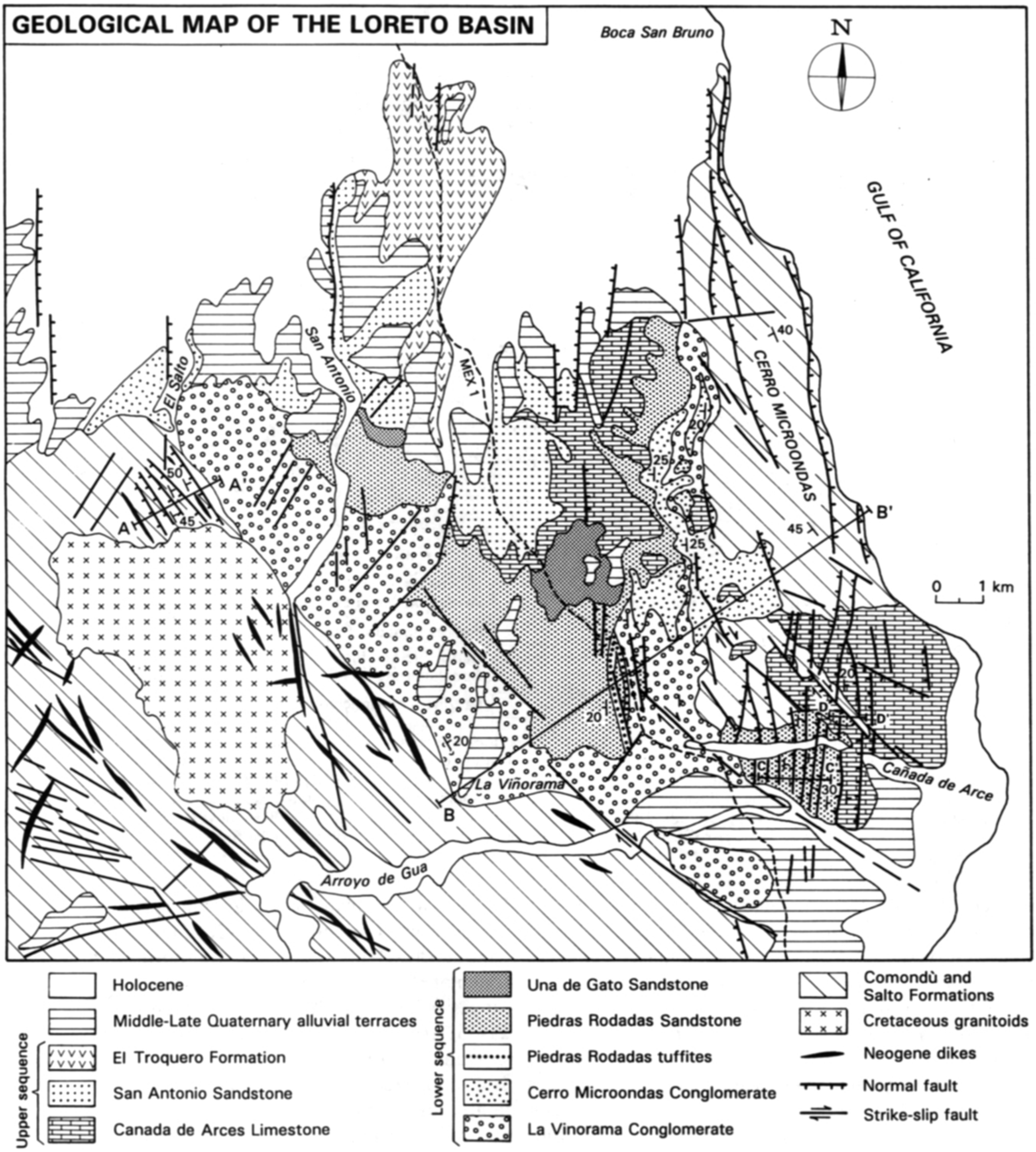

Fig. 9. Geological map of the Loreto basin. Map outline in Fig. 2.

plex kinematics, with strike-slip, oblique and, exceptionally, dip-slip motions. Compressive structures consisting in small E–W thrusts and folds were also observed, and indicate a N–S direction of the $\sigma 1$ axis.

In the southern part of the basin (Figs. 9 and 11) N–S normal west-dipping dip-slip faults have formed among NW–SE dextral-oblique strike-slip faults. The general geometric framework of this part of the basin suggests close relationships between the two different fault systems. The blocks containing N–S normal faults represent stepover structures formed among large dextral strike-slip faults. Deformation strongly increases within the stepovers, with bedding attitude reaching 45°, due to tilting along N–S normal faults. A schematic block-diagram of the structure present in the southern part of the basin has been reconstructed on the basis of the geometry of mapped faults outcropping along the Canada de Arces Sur (Fig. 12).

Most of the described structures can be considered very recent in time, because the top of the upper sequence of the Loreto basin is Late Pliocene–Early Pleistocene in age (Zanchi 1989b). Duration of tectonic activity until Late Pleistocene or Holocene is also suggested by motions along N–S trending normal faults

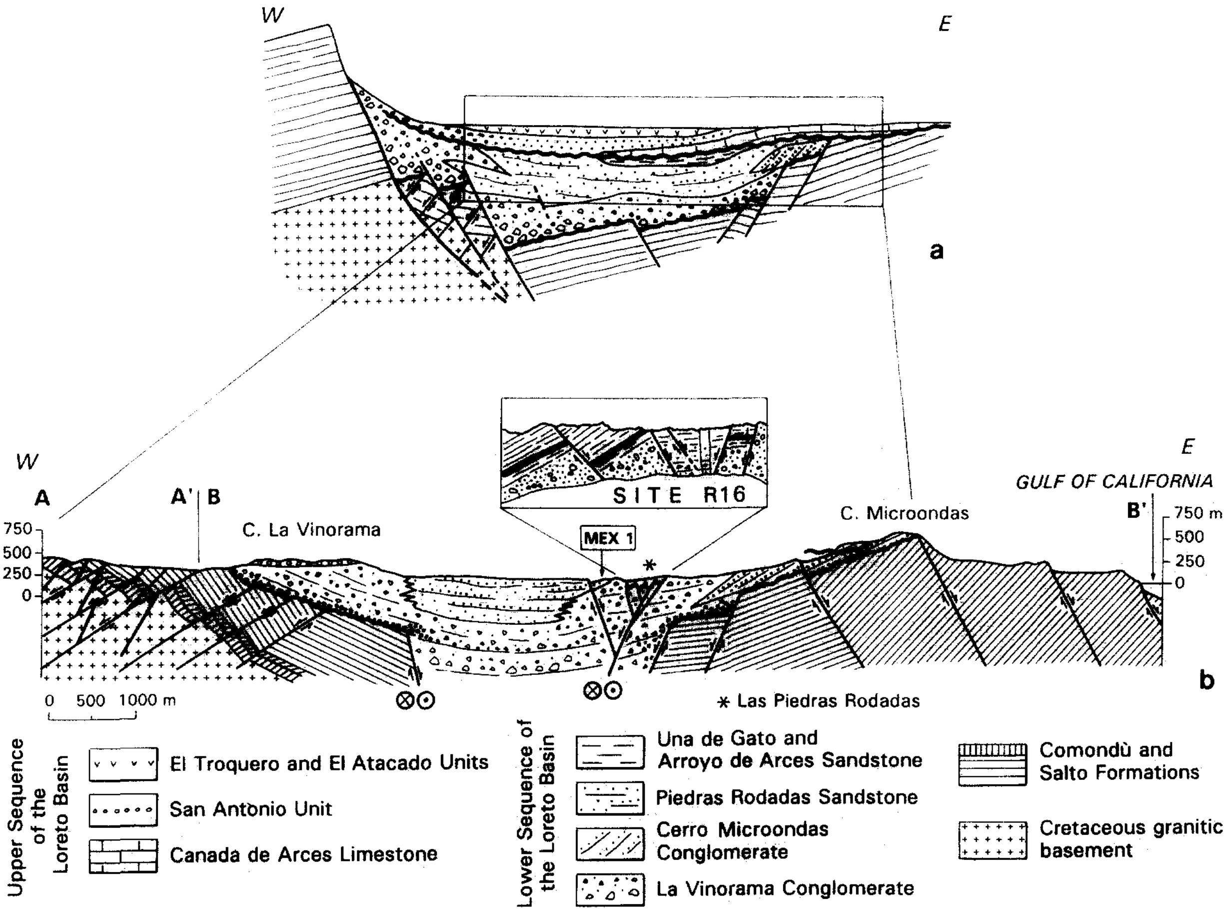

Fig. 10. Geological cross-sections through the Loreto basin. (a) Idealized, not to scale, stratigraphic and general structural framework of the Loreto basin. Post-sedimentary transtensional faults have been removed from the section. Note the unconformity separating the Comondù Formation from the lower sequence, and the one present between the upper and lower sequence. (b) Schematic geological cross-section through the southern part of the Loreto basin; see trace A–A'/B–B' in Fig. 9 for location. The small rectangle above the section relates to faults measured at site R16, near Rancho Piedras Rodadas, located along the Mex1 road. La Vinorama Conglomerate is stippled; Piedras Rodadas Sandstone is hatched; Piedras Rodadas tuffites are in solid black.

in recent alluvial terraces, where a recent change of the drainage pattern is evident. N–S normal faults and joints were observed also in a Quaternary marine terrace constituting the southern part of Isla Coronado, a small Pleistocene volcanic centre grown within the Gulf a few kilometres east of Loreto (Bigioggero *et al.* 1987).

A cross-section of Canada de Arces

In order to check the general consistency of the deformational system exposed in the southern part of the basin, a cross-section has been constructed using the E–W exposures of Canada de Arces, located a few kilometres north of Loreto. Here extensive outcrops have permitted the direct observation of fault motions and relative slips (Fig. 13). The section trends E–W and passes through an entire stepover, crossing also the strike-slip fault which bounds its northeastern margin. All the faults measured along the reconstructed section bear clear slip vectors and kinematic indicators, which are reported in Fig. 11. Sites R12, R13 correspond to the N–S trending normal fault within the stepovers. The major faults bounding the tilted blocks are mostly pure dip-slip (pitch between 75° and 90°), although also some normal oblique movements have been noticed on minor faults. Data relative to the dextral fault bounding the stepover are reported at site R26 (Fig. 11); this fault is dextral strike-slip with a dextral-normal component (pitch of 35° NW). The dip of bedding along the section ranges from about 30° to 45° increasing from west to east; it strongly decreases to about 20° east of the strike-slip fault. In some cases, the angle between the normal fault and bedding is about 90° along the N–S normal faults, suggesting a complex faulting history, with pre- and post-tilting motions (cf. Angelier & Colletta 1983).

Throws along the N–S trending normal faults have been observed in the field for most of the structures; the net throw of the strike-slip fault has been obtained evaluating its vertical offset and restoring the fault motion considering the slip vectors observed along the major fault plane. For this reason the obtained offset must be considered as an indicative value, because the observed striation may be only in part representative of the kinematic history of the fault. It is worth noting that the block east of the strike-slip fault shows a very different stratigraphic succession with respect to the one of the stepover, the main difference being the lack of several units of the Loreto basin. This can also indicate that the present-day strike-slip fault was possibly already active during sedimentation.

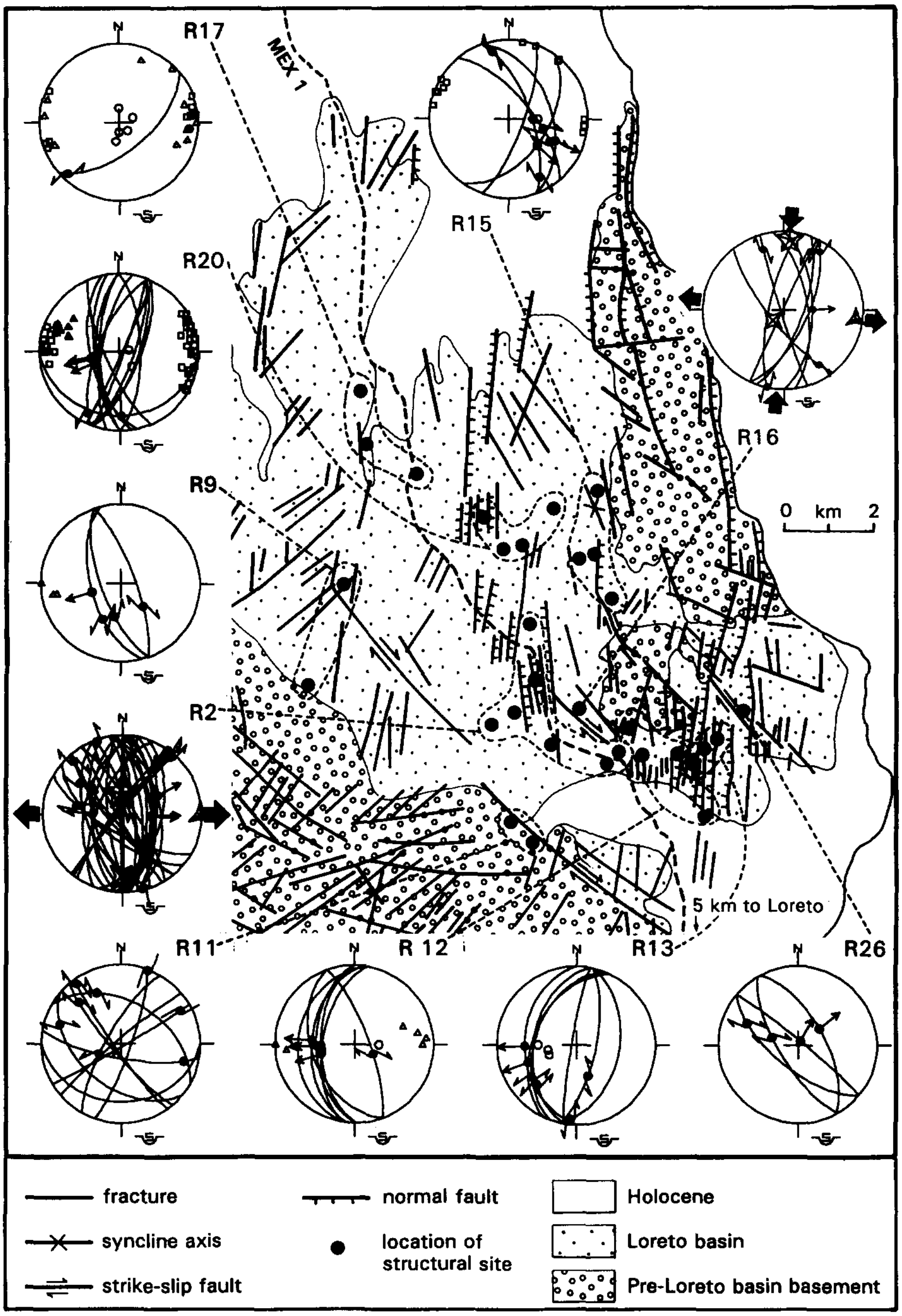

Fig. 11. Simplified structural map of the Loreto basin (see Fig. 9) and relative mesoscopic data. Squares are poles to tension gashes, triangles are poles to joints; structural data collected in each single site have been grouped in a few supersites.

Restoration of the section has been obtained moving the blocks backward along the observed slip-vectors, using simple trigonometry. Horizontal extension has been calculated using the formula for shortening percentage: $(L - L_0)/L_0 \cdot 100$ and it equals 45% for the entire section. The obtained cross-section can suggest further considerations regarding the kinematic interpretations of the analyzed structures. Let us consider the E–W extension produced by oblique motion along the NW–SE strike-slip oblique fault, and the E–W extension due to the N–S normal faults may be accommodation structures which form in order to balance the E–W extension created by strike-slip motions along NW–SE faults.

Aydin & Nur (1985) suggest that stepovers are fundamental and common features along important strike-slip faults. They correspond to en échelon segmentation of strike-slip faults which can occur both along the strike or along the dip of faults. Canada de Arces seems to be an along-strike stepover, because "strike-slip faults jump right or left but the faults are continuous in the dip directions" (Aydin & Nur 1985). Considering the many cases analyzed by these authors, the structures described in this paper are similar to the stepovers of type 2D–H (Aydin & Nur 1985 their fig. 2, p. 36), which form as accommodation structures relative to strike-slip faults with an original en échelon disposition. In this case, the en échelon disposition of strike-slip faults can be provided by the geometry of the faults related to the Protogulf opening, which have the same trend as the

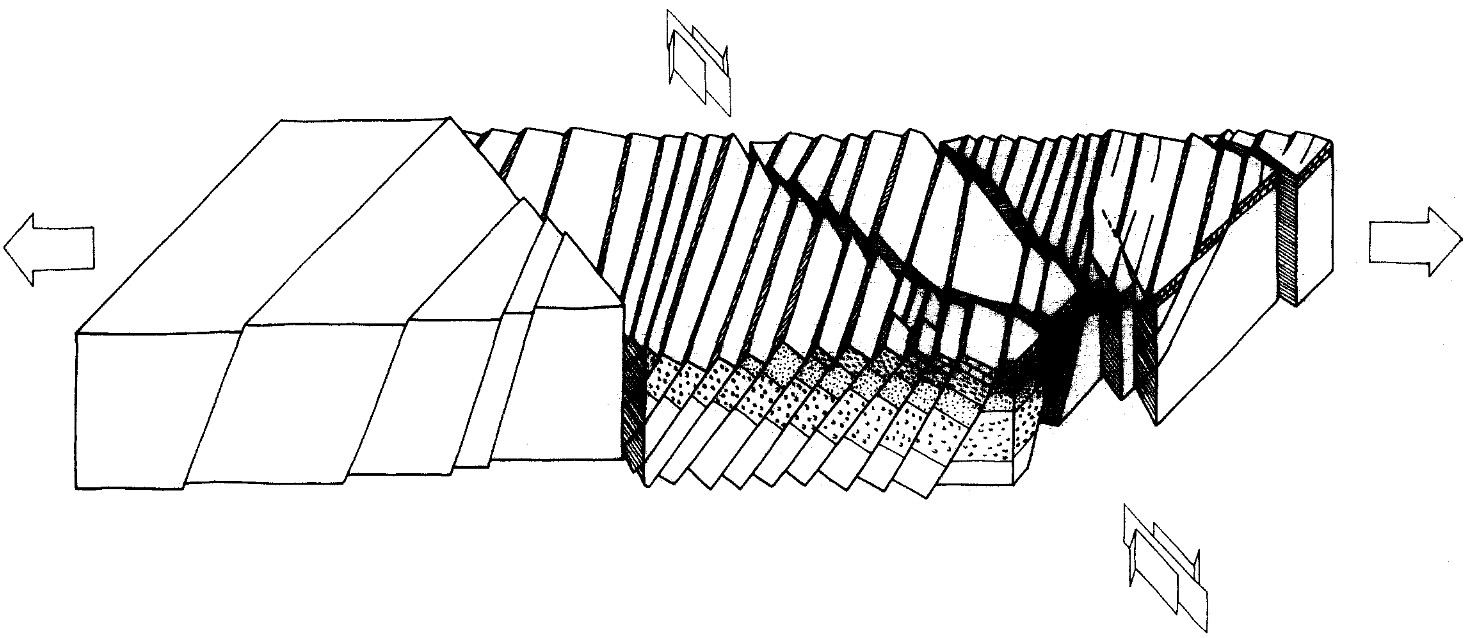

Fig. 12. Idealized, not to scale, block diagram relative to the extensional stepovers of Canada de Arces. The Comondù Formation, La Vinorama Conglomerate and the lower part of Piedras Rodadas Sandstone are in white; small circles, stipple and hatch correspond to the upper three units of the Piedras Rodadas Sandstone represented in the section of Fig. 13; brick is the Canada de Arces Limestone. Large divergent arrows indicate the direction of the $\sigma 3$ axis, which trends E–W; the direction of dextral shear is about NW–SE.

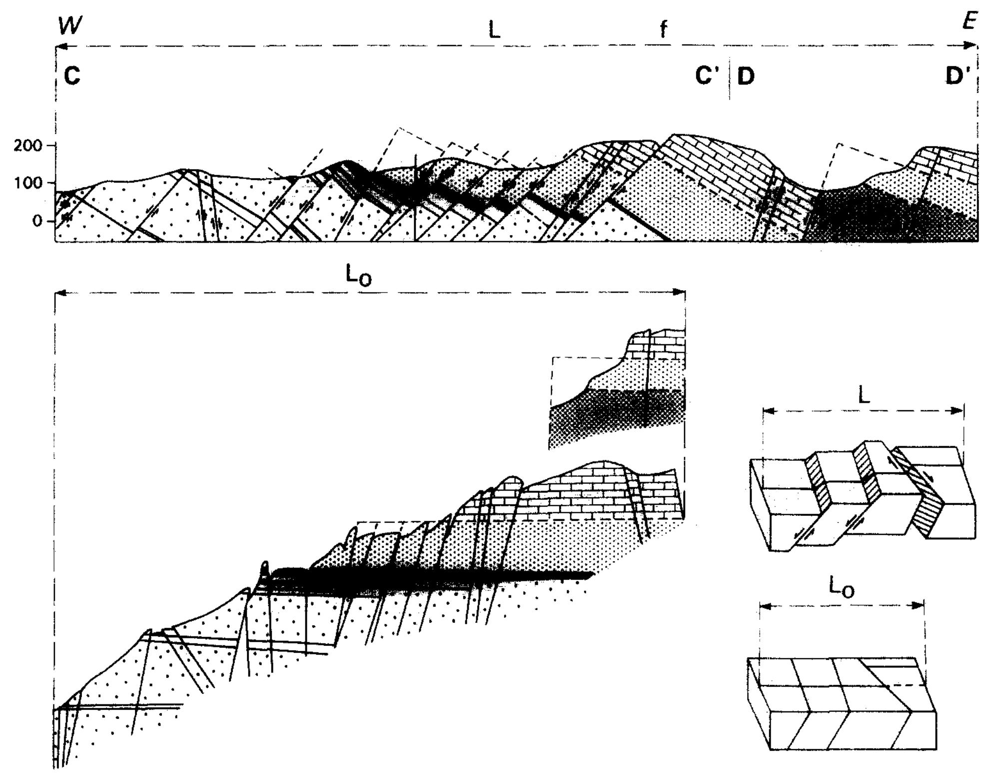

Fig. 13. Cross-section through Canada de Arces stepovers; the trace of the section is shown in Fig. 9 (C–C'/D–D'). Thick stippled corresponds to the Comondù Formation; large stippled corresponds to the disorganized sand and gravels of Piedras Rodadas Sandstone; solid black are conglomeratic layers regularly interbedded with sandstones (white) belonging to the same unit, medium stipple correspond to the sandstones of the top of Piedras Rodadas Unit; brick indicates the Canada de Arces Limestone. The two unconformities above the Comondù Formation and below the Canada de Arces Limestone are hatched. The small block diagrams on the right represents the process of restoration of the section, obtained moving back blocks along the slip vectors observed along fault planes.

dextral strike-slip faults of the Loreto basin. The Canada de Arces section differs from the Aydin & Nur (1985) models essentially because all of the normal faults preferentially show a strong westward dip which triggers the formation of uniformly tilted sectors, whereas Aydin & Nur (1985) predict the formation of symmetrical faults and deep pull-apart basins. This particular style is probably the result of complex processes involving the reactivation of the older Basin and Range structures, which control the formation of successive transtensional faults.

The total amount of extension along the stepover is about 25%, which is in good agreement with the results of Wernicke & Burchfield (1982, their fig. 10) about the extension produced by planar faults perpendicular to bedding.

Deformation in the Mencenares Volcanic Complex

The Mencenares Volcanic Complex (MVC) is a huge polyphase volcanic field developed a few kilometres east of the Main Gulf Escarpment during the opening of the Gulf of California (Fig. 14). The volcanic field has grown above a tilted and strongly dissected NW–SE trending horst, corresponding to the northward continuation of the Cerro Microondas structure. The main stratovolcano has formed inside a N–S graben, which clearly crosses the NW–SE Basin and Range horst.

The evolution of the volcanic area is described in detail by Bigioggero *et al.* (in review), and is characterized by several phases of activity, the last closely connected to a transtensional regime. During this phase, the main volcanic edifice (Cerro Mencenares) collapsed along N–S fault systems, leading to the formation of a large graben structure. The N–S faults acted also as a feeding system for the emplacement of andesitic–dacitic lava domes. Motions along the normal faults outlast this volcanic activity, causing tectonic deformation of flows and domes, whose explosive products are interfingered with the top of the upper sequence of the Loreto basin, supposed to be Early Pleistocene in age just south of the Mencenares stratovolcano (Zanchi 1989b).

Deformation is dominated by extension and the main mapped faults show normal slips, as in the case of the N–S system which crosscut the Cerro Mencenares (Fig. 14). In the northern part of the volcanic field the volcaniclastic sequences associated with the Cerro Mencenares activity are tilted up to 30°. The observed structures mainly fit the fault associations of the Loreto basin. Site S3 shows a full joint spectrum, including tension gashes, extensional, hybrid and shear joints, due to an active E–W $\sigma 3$ axis as in sites S5, S7, S9 and L1. Complex associations of vertical joints (S6 and L22) are present near some small domes, probably due to local disturbance in the stress field produced by magma emplacement at shallow depths.

STRESS PATTERNS AND STRUCTURAL EVOLUTION

Three main tectonic events were recognized in the Loreto area: (1) formation of large scale radial structures along the Main Gulf Escarpment during the last phases of the Comondù Arc activity; (2) NE–SW extension related to Basin and Range, associated with the formation of NW–SE faults with dip-slip motion; (3) transtension indicated by NW–SE dextral strike-slip faults and N–S dip-slip normal faults (Fig. 15).

Discussion and significance of the radial structures

Radial fracturing is related to a stress ellipsoid with a vertical $\sigma 1$ axis and a horizontal σh axis with no preferential orientation. This might explain the dispersion of the trends of the $\sigma 3$ axis within the radial structures (Table 1), due to the fact that eigenvalues are almost the same in every horizontal direction. The ratio Φ relative to the computed deviators supports this hypothesis, being very close to theoretical values for radial extension (Table 1). In such regimes the formation of normal faults with no preferential orientation has been inferred by Armijo *et al.* (1982).

Such a stress regime is known to be usually related to the presence of a circular hole filled with magma, as in the case of emplacement of magmatic bodies (Odé 1957, Robson & Barr 1964, Muller & Pollard 1977, Gerla 1988). On the contrary, Hyndman & Alt (1987) suggest that the presence of radial dike swarms associated with laccoliths can be explained as due to the weight of a huge volcanic apparatus dependent on a large feeder dike. The possible presence of thick piles of volcanics directly above the radial structures cannot be easily tested, because erosion has strongly affected the top of the Comondù Formation and the overlying volcanic successions. Nevertheless the dikes are intruded within volcaniclastic fluviatile sediments and at present no remnants of large volcanoes have been recognized on the mesas. In this way, the stress field induced by the emplacement of shallow magmatic bodies is a possible cause for the presence of radial structures.

According to Robson & Barr (1964), who propose a numerical model concerning the stress pattern near a circular magmatic chamber, the boundary stress conditions for the formation of radial structures of vertical dikes are: the presence of a vertical σmax, an internal pressure of magma equal to the σh and, finally, a tensile fracture zone must be present over the magmatic body. If the depth of the body is sufficient to produce a zone of shear fracturing, a caldera will form. The structural study performed in the Loreto region shows that both tensile and shear fracturing were active during the formation of the structures. In fact, in many cases the margins of the dikes bear striations or the dikes are crossed by normal fault planes parallel to the dikes themselves. These faults are consistent with the local stress field active during dike emplacement. Moreover, the subcircular fractures perpendicular to the radial systems may correspond to the circular faults of the model. In conclusion, tensile fracture could be active during the first stages of dike emplacement, while shear failure dominated afterwards. The same chronology of

(a)

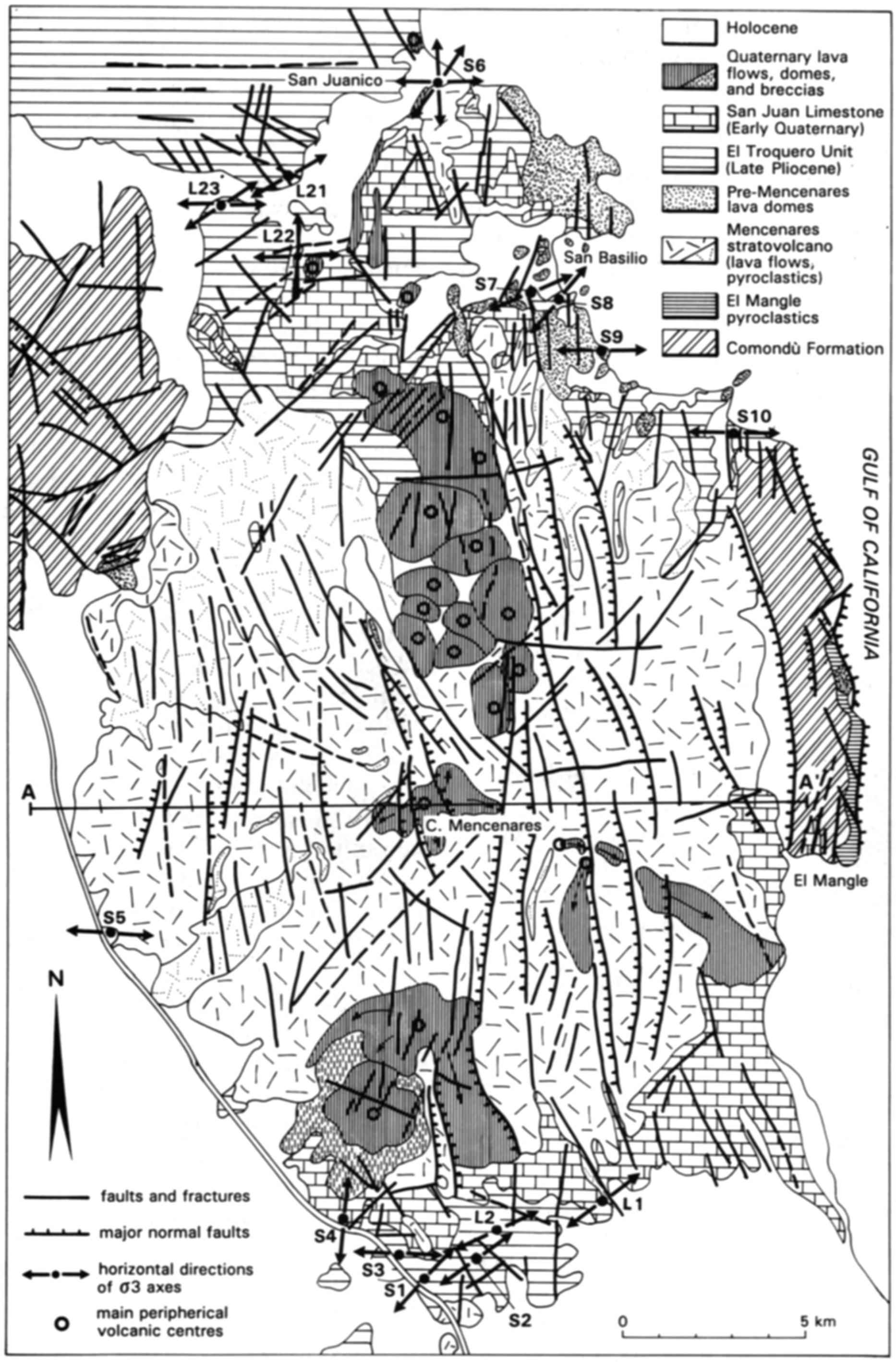

(b)

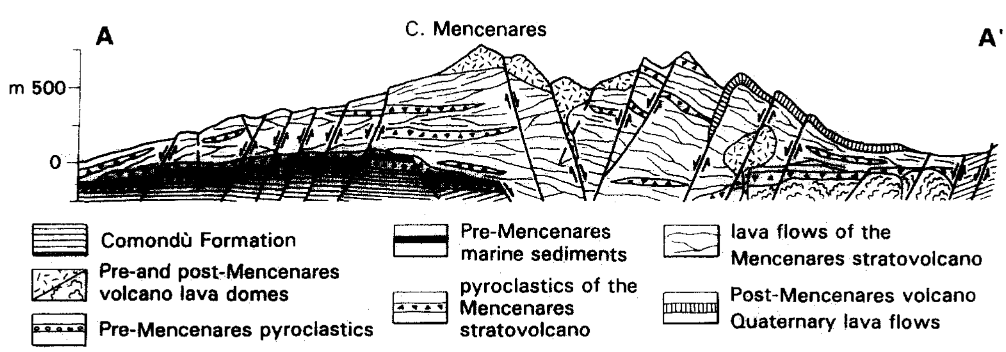

Fig. 14. (a) Geologic map of the Mencenares Volcanic Complex. (b) Geological cross-section through the Mencenares Volcanic Complex, A–A′ in (a). Map outline shown in Fig. 2.

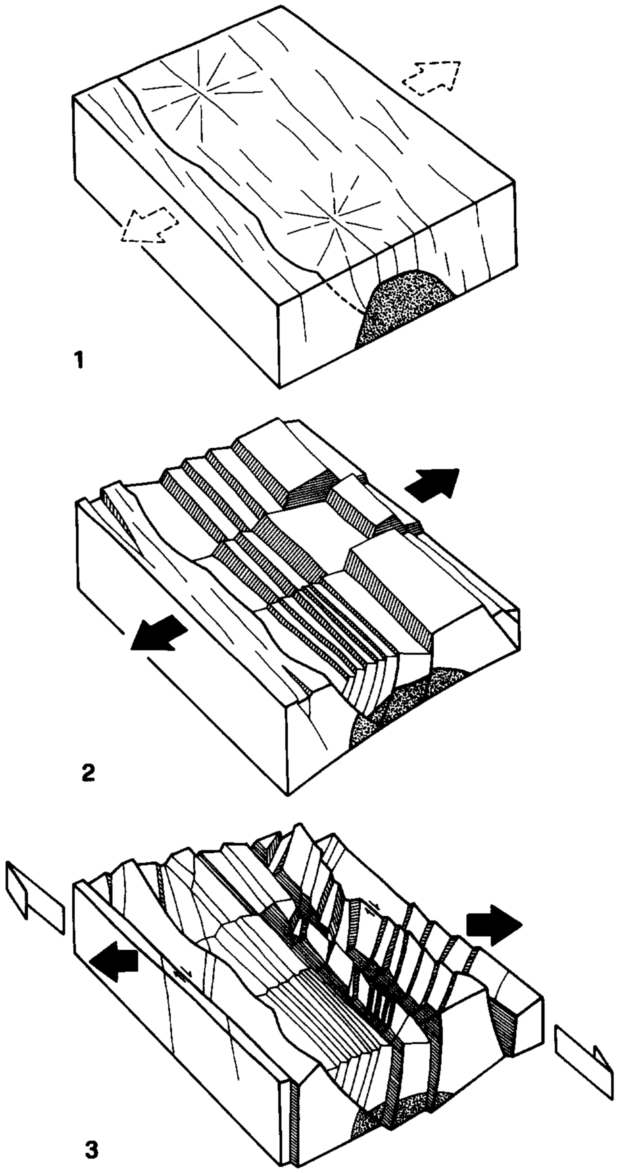

Fig. 15. Block-diagrams summarizing the tectonic evolution of the Loreto region. (1) Emplacement of magmatic bodies at shallow depth with formation of radial structures (Middle Miocene?) and possible beginning of NE–SW extension, (2) NE–SW extension with formation of Basin and Range 'style' structures related to the opening of the Protogulf of California (Late Miocene), and (3) transtension (Pliocene–Quaternary) associated with a clockwise rotation of the direction of extension from NE–SW to E–W, related to N–S compression and formation of large NW–SE dextral strike-slip faults.

failure mechanisms is also indicated by the mesoscopic fault analysis presented by Gerla (1988).

One of the most puzzling problems concerns timing of formation of the radial structures. In fact, west of Loreto the fracture systems of the Protogulf escarpment depart from a NW–SE strike and become subcircular, rotating around the Loreto radial structure. This may possibly suggest that the stress field related to the formation of radial structures was still active when Basin and Range extension began. On the other hand, the K/Ar ages of Gastil *et al.* (1979) and McLean (1988) concerning the dikes of the Loreto region cover a time span between 23 and 15 Ma. This age is much older than the age of 10 Ma indicated by many authors for the opening of the Protogulf. As already stated, the dikes cross a volcaniclastic sequence bearing the same or younger ages than those of the dikes. In counterpart, Hagstrum *et al.* (1987) obtained a poorly constrained age of 7.6 ± 5.5 Ma for an intrusive probably corresponding to the Pilon de las Parras subvolcanic body, one of the largest dikes of the Loreto radial structures, which was dated at 19 Ma by other authors (McLean 1988). Moreover, similar dike swarms crop out south of Loreto in a large tilted block downfaulted along the scarp, and cross the top of the Comondù sequences as well as some post-Comondù lava flows, generally dating around 15 Ma. One possible explanation for the different K/Ar ages is that several phases of dike emplacement with different structural positions and significance have occurred in the region. Some of the dated dikes, for instance, are intruded in the lower part of the Comondù Formation west of Loreto, and are different from the dikes associated with the radial systems which cut most of the Comondù succession.

Basin and Range extension

As suggested by relative fault chronology, the formation of radial structures and the emplacement of dike swarms was generally followed by the nucleation of the fracture system related to the Protogulf opening. Stress tensor determinations and fracture geometry indicate that during this event the $\sigma 1$ axis was vertical and the $\sigma 3$ axis had a NE–SW trend (Fig. 16a), producing NW–SE normal faults with characteristic pure dip-slip motions. The fracture field was uniform in the whole studied region and can be recognized in the interior of the peninsula up to the Pacific coast, where it is represented by vertical systems of closely spaced extensional joints and tension gashes developed within the sandstone of the Comondù Formation. Fault populations related to Basin and Range extension have been measured only in the volcaniclastics of the Comondù and Salto Formations, whereas they were not found in the sediments of the Loreto basin.

The development of the main escarpment might be partly conditioned by the stress field active within the radial structures, causing the main NNW–SSE to NW–SE fracture trends to deform, and giving rise to subcircular faults as in the case of those developed west of Loreto. This fact is enhanced at a mesoscopic scale by the presence of mixed assemblages of fault populations, including structures associated with both the events; fault populations also show the same type of slickensides and of growth fibres. Moreover, andesitic dikes with a strong affinity to those emplaced within the radial structures, and generally perpendicular to bedding planes, have NW–SE directions when emplaced far from these zones.

The studied area represents the westernmost termination of the Basin and Range Province. The Main Gulf Escarpment can be interpreted as a break-away ridge, whereas the coastal region corresponds to extensional allochthons. Here high rates of stretching are achieved in the upper crust through the formation of a peculiar counter-fan listric fault system moving on a detachment surface. According to Gibbs (1984), counter-fan geometry of tilted blocks is due to overpressures produced by high rates of sedimentation. Nevertheless, the strong angular unconformity between tilted blocks of the Comondù Formation and the debris-flows observed at the base of the lower sequence indicate that marine sedimentation was at least in part successive to the Protogulf formation.

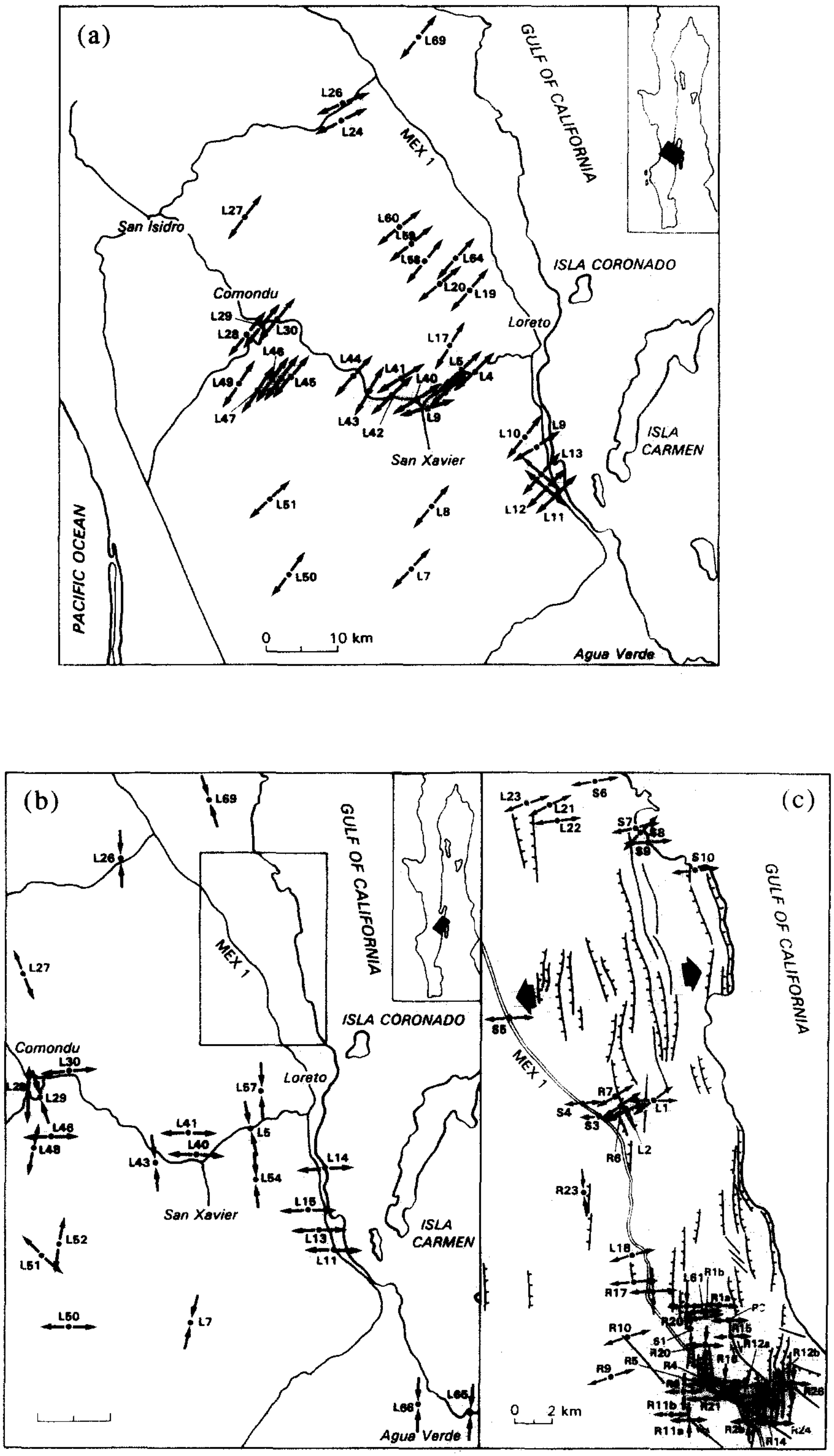

Fig. 16. Stress directions as deduced from fault analysis: (a) in the Comondù and Salto Formations during the opening of the Protogulf; (b) during transtension; and (c) in the Plio-Quaternary Loreto basin and in the Mencenares Volcanic Complex. Location of (c) is indicated in the rectangle in (b).

Transtension

Stress directions as deduced from fractures analysis in the Loreto basin indicate a regular pattern with a horizontal E–W $\sigma 3$ axis (Figs. 16b & c). Large NW–SE dextral strike-slip to oblique faults are associated with N–S normal faults with dip-slip motions, forming pull-apart basins and extensional stepovers. The strain produced by strike-slip motions is accommodated by extension along N–S normal faults, as indicated by geometrical relationships among faults in the southern part of the Loreto basin. This implies that strike-slip and normal faults seem to be strictly associated. The relative importance of strike-slip motion with respect to normal faulting is difficult to evaluate at a regional scale; although large NW–SE dextral strike-slip faults have been extensively mapped in the area, N–S trending normal faults are the most frequent structures observed in the Loreto basin and in the Mencenares Volcanic Complex.

Sedimentation in the Loreto basin seems to postdate the Basin and Range extension, as the lower sequence unconformably overlays, at least in the western part of the basin, NW–SE tilted blocks formed during the previous tectonic event. The Loreto basin can be interpreted as a large pull-apart structure (Zanchi *et al.* in progress) partly due to reactivation in a transtensional regime of the Basin and Range NW–SE normal faults. Also the Mencenares Volcanic Complex has grown along N–S trending structures, crossing previous NW–SE Basin and Range tilted blocks. High rates of E–W extension along normal faults are testified by the collapse of the early strato-volcano, which led to the formation of a N–S trending central graben filled with acidic lava flows. In this case hydromagmatic fracturing may have contributed to the activation of normal faults. The age of this structure is mainly Quaternary, as indicated by the interfingering of the volcanic products of the central graben with the top of the Loreto basin sediments.

The same stress directions have also been recognized in the Comondù and Salto Formations, and are mainly associated with the formation of conjugate sets of strike-slip faults, N–S trending normal faults and tension gashes (Fig. 16b). Inside the peninsula this tectonic regime is also testified by alignment of Quaternary volcanic centres, grown along N–S normal faults. Reactivation of the NW–SE normal faults of the Protogulf has been directly observed in the Comondù Formation volcaniclastics and can also be inferred by the original en échelon pattern of the NW–SE strike-slip faults of the southern part of the Loreto basin.

REGIONAL IMPLICATIONS AND CONCLUSIONS

The structural study performed in the Loreto region has led to the reconstruction of the paleostress fields and related deformational phenomena active during the opening of the gulf of California.

The emplacement at shallow depth of magmatic bodies can explain the presence of radial dikes and fractures, which developed along the future main escarpment of the rift in the southern part of Baja California from Bahia Conception to the Agua Verde area (Fig. 1). Intrusion of magmatic bodies at shallow depths during the early stages of rifting has been largely recognized in the Basin and Range Province (De Voogd *et al.* 1988, Gans *et al.* 1989, Meyer & Foland 1991). The dikes in the Loreto region have generally provided radiometric ages between 23 and 15 Ma (Gastil *et al.* 1979, McLean *et al.* 1987, McLean 1988). This indicates that extensional phenomena were active in the region a long time before the formation of the Protogulf rift, dated at 10 Ma in Baja California. Also Henry (1989) found in Sinaloa, Western Mexico, along the other side of the Gulf, NNW–SSE dikes with ages spanning between 32 and 24 Ma, whereas tilting and related faulting began only after 17 Ma. Demant *et al.* (1989) indicate that, in the Northern Sierra Madre Occidental, Basin and Range morphology was achieved between 20–17 Ma, while the strong 30–20 Ma volcanic activity was related to an important extensional phase which predates the development of Basin and Range structures. Although the connection of the radial structures with the beginning of Basin and Range extension seems probable, the available radiometric ages indicate an Early Miocene age for the emplacement of the radial swarm complexes, which could also be coincident with a late period of magmatic activity connected with the Comondù Arc of Hausback (1984).

The Basin and Range is represented by the nucleation of NW–SE dip-slip normal faults and joints, indicating a horizontal NE–SW trending $\sigma 3$ axis and a vertical $\sigma 1$ axis. Stress directions and fault populations are very similar to those described by Angelier *et al.* (1981) and Colletta & Angelier (1983) around the Santa Rosalia basin a few hundred kilometres to the north, suggesting a similar tectonic scenario. During this phase strongly tilted blocks with a characteristic counter-fan geometry formed east of the main scarp. High rates of extension due to crustal stretching can be inferred on the basis of the high rates of tilting. Basin and Range extension post-dates the effusion of 15 Ma lava flows dated by Gastil *et al.* (1979), and is post-dated by sedimentation in the Loreto basin. The Main Gulf Escarpment can be interpreted as the westernmost feature of the Basin and Range Province, whereas extensional phenomena strongly decrease inside the peninsula toward the Pacific margin. The presence of NW–SE trending dike swarms closely associated with the Basin and Range extensional structures indicate that dike emplacement in the region was a complex and polyphase event. The minimum age for the change from Basin and Range extension to transtension is indicated by the Plio-Quaternary Loreto basin sediments which, at least in part, overlie in a sharp angular unconformity the NW–SE trending tilted and extended blocks, and by the coeval volcanic activity of the Mencenares Complex.

Transtension has been largely recorded in the Loreto basin sediments and in the volcanics of the Mencenares

Complex. The most common fault assemblage is given by NW–SE dextral strike-slip to oblique faults and by N–S normal dip-slip faults. N–S faulting seems to be related to accommodation of the strain produced by motion along strike-slip faults. Similar fault populations have also been measured in the Comondù Formation, where reactivation of previous NW–SE normal faults with strike-slip motion is common. Stress directions indicate a regular stress field with a horizontal $\sigma 3$ axes, often associated along the Gulf coast to a horizontal $\sigma 1$ axis. This reconstruction is very similar to the paleostress field obtained by Angelier *et al.* (1981) along the peninsula. These authors suggest a more precise age for the beginning of transtension in the Santa Rosalia basin, where, in fact, the Late Miocene Boleo Formation unconformably covers Basin and Range tilted blocks. The NW–SE geometry of the Loreto basin and the disposition of NW–SE dextral strike-slip faults of the southern part of the basin confirm the importance of reactivation of the inherited Basin and Range structures in the development of dextral shearing along the Gulf of California.

Acknowledgements—The author is deeply indebted to Prof. J. Angelier (Université Paris VI, France) for his review and other helpful suggestions; stereoplots were drawn using his computer programs. I thank also Prof. J. Mercier (Université Paris Sud, France), Prof. Papani and Bernini (Dip. Scienze della Terra di Parma, Italy) for providing the computer program for stress tensor determination. Professor Pollard, Dr Treagus and an anonymous referee are also thanked for their precise and helpful observations. The work was supported with M.U.R.S.T. 40% funds. The author wishes to thank also his colleagues B. Biogioggero, S. Chiesa, S. Poli and A. Montrasio for the wonderful days spent together in the deserts of Baja California. G. Muttoni improved English in the final manuscript. Drawings were prepared by M. Minoli.

REFERENCES

Angelier, J. 1984. Tectonic analysis of fault slip data sets. *J. geophys. Res.* **89**, 5835–5848.

Angelier, J. & Colletta B. 1983. Tension fractures and extensional tectonics. *Nature, Lond.* **301**, 49–51.

Angelier, J., Colletta, B. & Anderson, R. E. 1985. Neogene paleostress changes in the Basin and Range: a case study at Hoover Dam, Nevada–Arizona. *Bull. geol. Soc. Am.* **96**, 347–361.

Angelier, J., Colletta, B., Chorowicz, J., Ortlieb, L. & Rangin, C. 1981. Fault tectonics of Baja California Peninsula and the opening of the Sea of Cortez, Mexico. *J. Struct. Geol.* **3**, 347–357.

Armigo, R., Carey, E. & Cisternas, A. 1982. The inverse problem in microtectonics and the separation of tectonic phases. *Tectonophysics* **82**, 145–160.

Atwater, T. 1970. Implications of plate tectonics for the Cenozoic tectonic evolution of Western North America. *Bull. geol. Soc. Am.* **81**, 3513–3536.

Aydin, A. & Nur, A. 1985. The types and roles of stepovers in strike-slip tectonics. *S.E.P.M.* 35–44.

Beal, C. H. 1948. Reconnaissance geology and oil possibilities of Baja California Peninsula. *GSA Memoir* **31**.

Bigioggero, B., Capaldi, G., Chiesa, S., Montrasio, A., Vezzoli, L. & Zanchi, A. 1987. Post-subduction magmatism in the Gulf of California: the Isla Coronado (Baja California Sur, Mexico). *Ist Lomb. Rend. Sc.* **B121**, 117–132.

Bischoff, J., Thomas, L. & Henyey, R. 1974. Tectonic elements of the central part of the Gulf of California. *Bull. geol. Soc. Am.* **85**, 1893–1904.

Boehm, M. C. 1984. An overview of the lithostratigraphy, biostratigraphy and paleoenvironments of the Late Neogene San Felipe marine sequence, Baja California, Mexico. In: *Geology of the Baja California Peninsula* (edited by Frizzel, V. A. Jr.). *Pacific Section S.E.P.M.* **39**, 253–265.

Carey, E. 1979. Recherche des directions principales de contraintes associées au jeu d'une population de failles. *Rev. Geol. Dyn. Geog. Phys.* **21**, 57–66.

Colletta, B. & Angelier, J. 1983. Tectonique cassante du Nord-Ouest Mexicain et ouverture du Golfe de Californie. *Bull. Cent. Rech. Explor. Prod. Elf Aquitaine* **7**, 433–441.

Couch, R. W., Ness, E. G., Sanchez-Zamorra, G., Calderon-Riverol, G., Dogiun, P., Plawman, T., Coperude, S., Huehm, B. & Gumma, W. 1991. In: *The Gulf and Peninsular Province of the Californias* (edited by Dauphin, J. P. & Simoneit, B. R. T.). *A.A.P.G. Memoir* **47**, 47–70.

Demant, A. 1984. The Reforma caldera, Santa Rosalia area, Baja California. A volcanological, petrological and mineralogical study. In: *Neotectonics and Sea Level Variations in the Gulf of California Area, a Symposium* (edited by Malpica, V., Celis, S., Guerrero, J. & Ortlieb, L.). *Univ. Nat. Auton. Mexico, Inst. Geologia, Mexico D.F.* 75–96.

Demant, A., Cochemé, J., Delpretti, P. & Piguet, P. 1989. Geology and petrology of the Tertiary volcanics of the northwestern Sierra Madre Occidental, Mexico. *Bull. Soc. géol. Fr.* **4**, 737–748.

De Voogd, B., Serpa, L. & Brown, L. 1988. Crustal extension and magmatic processes: COCORP profiles from Death Valley and the Rio Grande rift. *Bull. geol. Soc. Am.* **100**, 1550–1567.

Dokka, R. K. & Merriam, R. H. 1982. Late Cenozoic extension of northeastern Baja California, Mexico. *Bull. geol. Soc. Am.* **93**, 371–378.

Gans, P. B., Mahood, G. A. & Schermer, E. 1989. Synextensional magmatism in the Basin and Range province: a case study from the eastern Great Basin. *GSA Special Paper* **233**.

Gastil, R. G., Allison, E. C. & Phillips, R. 1975. Reconnaissance geology of the Baja California peninsula. *GSA Memoir* **140**.

Gastil, R. G., Krummenacher, D. & Minch, J. 1979. The record of Cenozoic volcanism around the Gulf of California. *Bull. geol. Soc. Am.* **90**, 839–857.

Gerla, P. J. 1988. Stress and fracture evolution in a cooling pluton: an example from the Diamond Joe stock, Western Arizona, U.S.A. *J. Volcanol. & Geotherm. Res.* **34**, 267–282.

Gibbs, A. D. 1984. Structural evolution of basin margins. *J. geol. soc. Lond.* **141**, 609–620.

Hagstrum, J., Sawlan, M., Hausback, B., Smith, J. & Grommé, C. 1987. Miocene Paleomagnetism and Tectonic Setting of the Baja California Peninsula, Mexico. *J. geophys. Res.* **92**, 2627–2639.

Hancock, P. 1985. Brittle microtectonics: principles and practice. *J. Struct. Geol.* **7**, 437–457.

Hausback, B. 1984. Cenozoic volcanic and tectonic evolution of the Baja California Peninsula. In: *Geology of the Baja California Peninsula* (edited by Frizzel, V. A. Jr.). *Pacific Section S.E.P.M.* **39**, 219–236.

Henry, C. D. 1989. Late Cenozoic Basin and Range structure in western Mexico adjacent to the Gulf of California. *Bull. geol. Soc. Am.* **101**, 1147–1156.

Hyndman, D. W. & Alt, D. 1987. Radial dikes and gelatin models. *J. Geol.* **95**, 763–774.

Karig, D. E. & Jensky, W. 1972. The Protogulf of California. *Earth Planet. Sci. Lett.* **17**, 169–174.

Klitgord, K., Mudie, J., Bischoff, J. & Henyey, T. 1974. Magnetic anomalies in the northern and central Gulf of California. *Bull. geol. Soc. Am.* **85**, 815–820.

Larsen, P. H. 1988. Relay structures in a Lower Permian basement-involved extension system, East Greenland. *J. Struct. Geol.* **10**, 3–8.

Larson, R. L., Menard, H. W. & Smith, S. 1968. Gulf of California: a result of ocean floor spreading and transform faulting. *Science, N.Y.* **161**, 881–884.

Larson, R. 1972. Bathymetry, magnetic anomalies and plate tectonic history of the mouth of the Gulf of California. *Bull. geol. Soc. Am.* **83**, 3345–3360.

Larson, P., Mudil, J. & Larson, R. 1972. Magnetic anomalies and fracture zone trends in the Gulf of California. *Bull. geol. Soc. Am.* **83**, 3361–3368.

Lonsdale, P. 1991. Structural patterns of the Pacific floor off-shore of Peninsular California. In: *The Gulf and Peninsular Province of the Californias* (edited by Dauphin, J. P. & Simoneit, B. R. T.). *A.A.P.G. Memoir* **47**, 87–126.

Lyle, M. & Ness, G. E. 1991. The opening of the southern Gulf of California. In: *The Gulf and Peninsular Province of the Californias* (edited by Dauphin, J. P. & Simoneit, B. R. T.). *A.A.P.G. Memoir* **47**, 403–424.

Mammerickx, J. & Klitgord, K. 1982. Northern East Pacific Rise evolution from 25 m.y. b.p. to the present. *J. geophys. Res.* **87**, 6751–6759.

McFall, C. 1968. Reconnaissance geology of the Conception bay area. Baja California. *Univ. Stanf. Pubs geol. Sci.* **10**, 1–25.

McLean, H. 1988. Reconnaissance geologic map of the Loreto and part of the San Javier quadrangles, Baja California Sur, Mexico. *U.S. Geol. Surv. Misc. Field Stud. Map, MF-1799.*

McLean, H., Hausback, B. & Knapp, J. H. 1987. The Geology of West-Central Baja Californa Sur, Mexico. *Bull. U.S. geol. Surv.* **1579**.

Meyer, J. & Foland, K. A. 1991. Magmatic-tectonic interaction during early Rio Grande rift extension at Questa New Mexico. *Bull. geol. Soc. Am.* **103**, 993–1006.

Moore, D. 1973. Pliocene deformation and crustal growth, Gulf of California structural province. *Bull. geol. Soc. Am.* **84**, 1883–1906.

Moore, D. & Buffington, E. 1968. Transform faulting and growth of the Gulf of California since late Pliocene. *Science, N.Y.* **61**, 1238–1241.

Muller, O. H. & Pollard, D. D. 1977. The stress state near Spanish Peaks, Colorado determined from a dike pattern. *Pure & Appl. Geophys.* **115**, 69–86.

Odé, H. 1957. Mechanical analysis of the dike pattern of the Spanish Peaks area, Colorado. *Bull. geol. Soc. Am.* **68**, 567–576.

Ortlieb, L. & Colletta, B. 1984. Sintesis cronoestratigrafica sobre el Neogeno y el Cuaternario Marino de la cuenca de Santa Rosalia, Baja California Sur, Mexico. In: *Neotectonics and Sea Level Variations in the Gulf of California Area, a Symposium* (edited by Malpica, V., Celis, S., Guerrero, J. & Ortlieb, L.). *Univ. Nat. Auton. Mexico, Inst. Geologia, Mexico D.F.*

Ortlieb, L., Ruegg, J. C., Angelier, J., Colletta, B., Kasser, M. & Lesage, P. 1989. Geodetic and tectonic analyses along an active plate boundary: the central Gulf of California. *Tectonics* **8**, 429–441.

Petit, J. 1987. Criteria for the sense of movement on fault surfaces in brittle rocks. *J. Struct. Geol.* **9**, 597–608.

Robson, G. R. & Barr, K. G. 1964. The effect of stress on faulting and minor intrusions in the vicinity of a magma body. *Bull. Volc.* **29**, 315–330.

Rusnack, G., Fisher, R. & Shepard, F. P. 1964. Bathymetry and faults of the Gulf of California. In: *Marine Geology of the Gulf of California; a Symposium* (editors van Andel, T.H. & Shor, G. G.). *AAPG Memoir* **3**, 59–75.

Saunders, A. D., Rogers, G., Marriner, G. F., Terrell, D. J. & Verma, S. P. 1987. Geochemistry of Cenozoic volcanic rocks, Baja California, Mexico: implications for the petrogenesis of post-subduction magmas. *J. Volcanol. & Geotherm. Res.* **32**, 223–245.

Sawlan, M. C. & Smith, J. C. 1984. Petrologic characteristics, age and tectonic setting of Neogene volcanic rocks in Northern Baja California Sur. In: *Geology of the Baja California Peninsula* (edited by Frizzel, V. A. Jr.). *Pacific Section S.E.P.M.* **39**, 237–251.

Smith, J. T. 1991. Cenozoic marine molluscs and paleogeography of the Gulf of California. In: *The Gulf and Peninsular Province of the Californias* (edited by Dauphin, J. P. & Simoneit, B. R. T.). *A.A.P.G. Memoir* **47**, 637–666.

Spencer, J. & Normark, W. 1979. Tosco-Abreojos fault zone: a Neogene transform plate boundary within the Pacific margin of southern Baja California. *Geology* **7**, 554–557.

Stock, J. M. & Hodges, K. V. 1989. Pre-Pliocene extension around the Gulf of California and the transfer of Baja California to the Pacific Plate. *Tectonics* **8**, 99–115.